Aurora-A mediated histone H3 phosphorylation of threonine 118 controls condensin I and cohesin occupancy in mitosis

Candice L. Wike[1], Hillary K. Graves[1], Reva Hawkins[1], Matthew D. Gibson[2], Michelle B. Ferdinand[3], Tao Zhang[4], Zhihong Chen[1], Damien F. Hudson[4], Jennifer J. Ottesen[3], Michael G. Poirier[2], Jill Schumacher[5], Jessica K. Tyler[1,6*]

[1] Department of Epigenetics and Molecular Carcinogenesis, University of Texas MD Anderson Cancer Center, Houston, Texas 77030, USA.

[2] Department of Physics Ohio State University, Columbus, OH 43210, USA.

[3] Department of Chemistry and Biochemistry, Ohio State University, Columbus, OH 43210, USA.

[4] Murdoch Children's Research Institute, Royal Children's Hospital, Melbourne, Victoria 3052, Australia.

[5] Department of Genetics, University of Texas MD Anderson Cancer Center, Houston, Texas 77030, USA.

[6] Current address: Department of Pathology and Laboratory Medicine, Weill Cornell Medicine, 1300 York Ave, New York, NY 10065.

[*] To whom correspondence should be addressed: jet2021@med.cornell.edu

Short title: Aurora-A mediated phosphorylation of H3

Keywords: Aurora-A, histone H3 phosphorylation, cohesion, condensin, chromosome congression

Abstract

Phosphorylation of histone H3 threonine 118 (H3 T118ph) weakens histone DNA-contacts, disrupting the nucleosome structure. We show that Aurora-A mediated H3 T118ph occurs at pericentromeres and chromosome arms during prophase and is lost upon chromosome alignment. Expression of H3 T118E or H3 T118I (a SIN mutation that bypasses the need for the ATP-dependent nucleosome remodeler SWI/SNF) leads to mitotic problems including defects in spindle attachment, delayed cytokinesis, reduced chromatin packaging, cohesion loss, cohesin and condensin I loss in human cells. In agreement, overexpression of Aurora-A leads to increased H3 T118ph levels, causing cohesion loss, and reduced levels of cohesin and condensin I on chromatin. Normal levels of H3 T118ph are important because it is required for development in fruit flies. We propose that H3 T118ph alters the chromatin structure during specific phases of mitosis to promote timely condensin I and cohesin disassociation, which is essential for effective chromosome segregation.

Introduction

The packaging of the eukaryotic genome into chromatin facilitates the temporal and spatial regulation of all genomic activities, including DNA repair, replication, transcription and mitosis. Chromatin comprises arrays of nucleosomes, where each nucleosome has ~146 base pairs of DNA wrapped 1.75 times around a histone octamer composed of two molecules each of core histone H3, H4, H2A, and H2B (Kornberg 1974). Repetitive arrays of nucleosomes are then further compacted by higher-order folding, requiring additional proteins including linker histones. During mitosis, chromosome condensation plays a critical role in preventing DNA breaks during mitosis and enabling equal chromosome segregation to the two daughter cells (Ganem and Pellman 2012).

One important means by which the cell achieves accurate regulation of genomic processes, including mitosis, is via post-translational modifications (PTMs) of the core histones (Strahl and Allis 2000). The PTMs, usually occurring on the N- and C-terminal tails of the histones, generally serve to recruit reader proteins to the chromatin. PTMs also occur on the histone globular domains, but are much less well studied than the histone tail modifications. PTMs at the histone-DNA interface have been proposed to directly modulate nucleosome structure, without the need for reader proteins (Cosgrove, Boeke et al. 2004). Of all the histone PTMs that occur at the histone-DNA interface, one of the best positioned to disrupt the nucleosome structure is phosphorylation of threonine 118 (T118ph) of H3 (Mersfelder and Parthun 2006). In agreement with its important location within the nucleosome structure (Figure 1A), biochemical studies have confirmed that H3 T118ph causes reduced nucleosome stability, increased nucleosome mobility, and increased DNA accessibility (North, Javaid et al. 2011). Strikingly, H3 T118ph caused the formation of novel populations of alternate DNA-histone

complexes that have DNA wrapped around two complete histone octamers arranged edge-to-edge, termed nucleosome duplexes and altosomes (North, Simon et al. 2014). In agreement with the biochemical data, a substitution of H3 T118 for isoleucine (T118I) was identified in *S. cerevisiae* as a dominant Swi-INdependent (SIN) (Kruger, Peterson et al. 1995). The SIN H3 T118I substitution allows nucleosomes to slide along the DNA without the need for SWI/SNF (Muthurajan, Bao et al. 2004).

Despite the striking biochemical effects of H3 T118ph on nucleosome structure and the phenotype of the yeast T118I mutant, H3 T118ph has not been studied in cells beyond its identification (Olsen, Vermeulen et al. 2010). Accordingly, we characterized H3 T118ph function in metazoan cells. H3 T118ph, mediated by Aurora-A, is localized to centromeres and chromosome arms during specific phases of mitosis, Mutation of H3 T118 caused a wealth of defects including lagging chromosomes, delayed cytokinesis, reduced cohesion and altered chromosome compaction in mammalian cells and inviability in *Drosophila*. Given that the H3 T118I mutant or overexpression of Aurora-A led to premature release of cohesin and condensin I from chromosomes, we propose that H3 T118ph alters chromosome structure during mitosis to help dissociate cohesion and condensin I.

Results

H3 T118ph is dynamically regulated during mitosis in metazoans

To characterize the spatiotemporal localization of H3 T118ph (Figure 1A), we first established the specificity of the H3 T118ph antibodies. Here we show only the results obtained with the Abcam antibody, although similar results were obtained with our independently generated H3 T118ph polyclonal antisera (data not shown). The antisera were highly specific in dot-blot assays (Figure 1B) and recognize a single protein identical in size to histone H3 in western blot analysis of total protein extracts from HeLa cells (Figure 1C). This signal in western blots was increased by treating the cells with the protein phosphatase 1 and 2A inhibitor calyculin A for 3 hours, indicating that the H3 T118ph antibody recognized phosphorylated H3 (Figure 1D, Figure 1 – figure supplement 1A). In concordance with previously published mass spectrometry results (Olsen, Vermeulen et al. 2010), we observed a dramatic increase in H3 T118ph levels as cells entered mitosis (Figure 1E). The antibody also recognized H3 T118ph in its native conformation, because it immunoprecipitated H3 from cells released into mitosis (Figure 1F, Figure 1 – figure supplement 1B). Using immunofluorescence analysis, we found that H3 T118ph was restricted to mitotic cells during prophase through anaphase and was greatly diminished in interphase (Figure 1G). Specifically, H3 T118ph signal was detected as discrete foci on chromatin only in prophase and pro-metaphase. Additionally, H3 T118ph co-localized with centrosomes through all phases of mitosis (Figure 1G). This is a consequence of non-chromatin bound histones localizing to the centrosomes for proteasome-mediated degradation during mitosis (C. Wike and J.K. Tyler, manuscript submitted). During anaphase, the H3 T118ph antibodies also detected the spindle mid-body (Figure 1G). The localization pattern of H3 T118ph was not unique to HeLa cells, nor cancer cell lines, because it was similar in HMEC, WI-38 and MCF10A cells (data not shown). Finally, the H3 T118ph signal

was specifically competed away by an H3 T118ph peptide (Figure 1H). Together, these results show that the H3 T118ph antibody is specific.

H3 T118ph localizes to centromeres and chromosome arms during prophase and pro-metaphase

Threonine 118 and the surrounding residues are highly conserved among metazoan H3 proteins. Therefore, we tested whether H3 T118 is phosphorylated in other metazoans and whether this occurs specifically during mitosis. In *D. melanogaster* S2 cells, H3 T118ph localized to chromatin and centrosomes during mitosis (data not shown). H3 T118ph localization was also conserved in *C. elegans*. During pro-metaphase, H3 T118ph was localized along the outside edges of chromosomes, indicative of centromeric localization on holocentric chromosomes in *C. elegans* (Figure 2A). To determine if the localization of H3 T118ph along the arms of chromosomes was dependent on the centromeric chromatin structure, we used siRNA to the centromeric histone variant CENP-A to abolish the centromeres. Upon CENP-A knockdown, H3 T118ph is diminished from the chromatin (Figure 2A). These data demonstrate that mitotic enrichment of H3 T118ph is conserved amongst metazoans. Furthermore, H3 T118ph localizes to centromeres and its localization is dependent on intact centromeres.

Given our results in *C. elegans*, we asked if the punctate chromosomal staining of H3 T118ph in mammalian cells (Figure 1G) reflects centromeric staining. Indeed, we found that H3 T118ph co-localized with CENP-A in human cells in prophase and pro-metaphase (Figure 2B). Noteworthy, the prophase to metaphase timing of the appearance and disappearance of H3 T118ph on centromeres is distinct from other mitotic H3 phosphorylation events. For example, H3 S10ph (Crosio, Fimia et al. 2002) and H3 T3ph (Polioudaki, Markaki et al. 2004)

remain on chromosome arms and centromeres, respectively, through anaphase. CENP-A S7ph (Zeitlin, Shelby et al. 2001) remains through metaphase, while H3 T118ph is lost from centromeres in metaphase coincident with chromosome alignment. H3 T118ph foci did not always perfectly colocalize with CENP-A, but sometimes appeared to be adjacent to CENP-A foci. Indeed, detailed inspection of mitotic spreads revealed that H3 T118ph localized to the inner centromere when cells were treated with the microtubule destabilizing drug colcemid while CENP-A remained on the outer-centromere (Figure 2C). The distinct localization of CENP-A and H3 T118ph emphasizes that the H3 T118ph signal is not due to phosphorylation of CENP-A *per se*. Importantly, upon colcemid treatment, where microtubule attachment is lost, the interkinetochore distance is decreased (Uchida, Takagaki et al. 2009). The single foci that is detected by H3 T118ph antibody could be because of a single population of H3 T118ph localized to the inner-centromere or because the two adjacent centromeres are separated by less than the resolution of light microscopy, which is theoretically 200nm. Therefore we asked when there is dynamic microtubule attachment, promoting tension and kinetochore stretching, what is the true H3 T118ph signal at the centromere. H3 T118ph existed in two foci per chromosome that correlate well with, but are larger than, the two CENP-A foci (Figure 2D) consistent with pericentromeric localization. We noted that H3 T118ph also appears to occur along the chromosome arms in mitotic spreads (Figure 2D). Indeed, H3 T118ph was detectable at the centromere partially overlapping with CENP-A and at weaker foci at discrete intervals along the chromosome arms on extended chromatin fibers (Figure 2E).

Aurora-A phosphorylates H3 T118

To gain insight into the function of H3 T118ph, we sought to identify the kinase responsible for its phosphorylation. We utilized a ProQinase kinase screen to test 190 recombinant

kinases for their ability to phosphorylate H3 T118 (Figure 3 – figure supplement 1). Aurora-A was the only cell cycle regulated kinase able to efficiently phosphorylate H3 T118 from among the three positive kinases, arbitrarily defined as having an activity above 3000 cpm. Absence of phosphorylation of H3 T118 by Aurora-B and Aurora-C further validated Aurora-A as the kinase of H3 T118 (Figure 3A). We independently confirmed that Aurora-B INCENP could not phosphorylate the T118 peptide, including an H3 S10 peptide as a positive control (data not shown). Two different inhibitors to Aurora-A eradicated the H3 T118ph signal (Figure 3 – figure supplement 2A). Upon Aurora-A knockdown, which eradicated most of the Aurora-A protein and activity (Figure 3 – figure supplement 2B, Figure 3 – figure supplement 3A), H3 T118ph was undetectable on chromatin (Figure 3B). In agreement with Aurora-A being the *bona fide* H3 T118 kinase, knockdown of TPX2, a known activator of Aurora-A (Kufer, Sillje et al. 2002), greatly reduced H3 T118ph (Figure 3 – figure supplement 3B,C). Taken together, these results demonstrate that Aurora-A mediates H3 T118 phosphorylation.

H3 T118I and T118E increase lagging chromosomes and chromosome alignment errors

Given that H3 T118ph is detectable on chromatin during early mitosis (Figure 1G, 2B), we investigated whether H3 T118ph plays a role in mitotic progression. To do this, we mutated T118 to alanine to prevent its phosphorylation. This serves as a negative control that is not expected to yield a phenotype, because there is still phosphorylation of the endogenous H3. We also mutated T118 to glutamic acid (E), although this mutation does not cause the nucleosome destabilization or altered nucleosome structures that result from T118 phosphorylation *in vitro* (North, Javaid et al. 2011, North, Simon et al. 2014). As such, T118E is not an effective mimic of T118 phosphorylation, at least on mononucleosomes *in vitro*. We also mutated H3 T118 to isoleucine (I) to recapitulate the yeast sin mutant. Transient

transfection of HEK 293TR cells with plasmids expressing histone H3:YFP where T118 was mutated to E or I led to a significantly increased incidence of lagging chromosomes (Figure 3C,D). Equal expression of the wild type and mutant H3 proteins was verified by western blot analysis (Figure 3 – figure supplement 4A). Using time-lapse microscopy, we found that cells expressing H3 T118E:YFP or H3 T118I:YFP had significant delays in cytokinesis (Figure 3E**,** Figure 3 – figure supplement 4B**,** see material and methods). Furthermore, whenever a lagging chromosome was evident, there also was an accompanying delay in the subsequent cytokinesis, regardless of the transfected construct (Figure 3 – figure supplement 4C). From these experiments, we conclude that expression of H3 T118I and T118E results in lagging chromosomes that delay cytokinesis.

An increase in lagging chromosomes is symptomatic of defects in chromosome congression (Thompson and Compton 2011). This prompted us to investigate if phosphorylation of H3 T118 plays a role in correction of chromosome alignment errors, using an error correction assay (Lampson, Renduchitala et al. 2004, Santaguida, Tighe et al. 2010). For this, we created a panel of stable 293TR cell lines expressing FLAG-tagged wild type H3, H3 T118E, T118I, or T118A from the same locus. All the H3:FLAG proteins were expressed to equivalent levels, at approximately 10% of the endogenous H3 level (Figure 3 – figure supplement 4D,E) and all could be incorporated into chromatin (Figure 3 – figure supplement 5A). We further verified that the H3 T118 mutations in H3:FLAG did not cause a delay in prophase to anaphase (Figure 3 – figure supplement 5B). The error correction assay was as follows: Monastrol was used to induce a monopolar spindle and kinetochore-microtubule attachment errors (Figure 3F). The cell lines were able to recover by washing out Monastrol if proper checkpoints and machinery are in place and the chromosomes will attach to bipolar spindles. Additionally, cells were released in the presence of MG132 to allow time to align the

chromosomes to the metaphase plate by preventing cells from entering anaphase. Importantly, the H3 T118 mutations did not delay release from the pro-metaphase arrest (Figure 3 – figure supplement 5C). Expression of either H3 T118E or T118I significantly decreased the ability to align chromosomes compared to wild type H3 or T118A (Figure 3F,G). This result suggests that an over abundance of H3 T118E and T118I mutants may hinder chromosome congression.

Normal levels of H3 T118 phosphorylation are essential for development

Our results suggest an important role for phosphorylation of H3 T118 in regulating chromosomal dynamics in metazoans. However, these studies were performed in a situation where only 10% of the histone H3 was mutant. In order to examine the consequences of having all or none H3 phosphorylated on T118, we introduced the T118 mutations into 12 copies of the H3 gene on transgenes and introduced them into *Drosophila* where the endogenous H3 gene copies were deleted (Figure 3 – figure supplement 6A), such that the flies only expressed H3 T118A, T118E, or T118I (Gunesdogan, Jackle et al. 2010). While control animals bearing wild type H3 survived to adulthood, animals expressing the mutant H3 T118A, E and I died as embryos after depletion of the maternal contribution of histones (Figure 3 – figure supplement 6B). These results indicate that normal levels of H3 T118ph are essential for development.

H3 T118ph remains at misaligned chromosomes

Having found that phosphorylation of H3 T118 was essential for development in fruit flies, we sought to gain a better understanding of its function. Since cells expressing H3 T118I and T118E showed reduced chromosome congression, we asked if H3 T118ph remains at centromeres of misaligned chromosomes as the cells enter metaphase. Caffeine was used to

induce misaligned chromosomes (Katsuki, Nakada et al. 2008). H3 T118ph remained at centromeres of misaligned chromosome along with the spindle assembly checkpoint (SAC) kinase BubRI, even in metaphase (Figure 4A). This suggests that removal of H3 T118ph is triggered by chromosome alignment and led us to speculate that H3 T118ph plays a role in achieving efficient chromosome attachment. Accordingly, we investigated the potential molecular reasons for the defect in chromosome congression caused by H3 T118E and T118I. Outer-kinetochore proteins, spindle assembly checkpoint proteins and the heterochromatin landscape were indistinguishable between cells expressing H3 T118A, T118E, T118I or wild type H3 (data not shown). Taken together, these data show that misaligned chromosomes in H3 T118I and T118E mutants are capable of forming proper kinetochores and recruiting SAC proteins

Loss of cohesion due to excess H3 T118ph

Because sister chromatid cohesion is important for chromosome congression, we examined whether the H3 T118I or T118E mutations caused faulty cohesion. Mitotic spreads from cells expressing wild type H3 or H3 T118A upon pro-metaphase arrest (induced by Monastrol) and metaphase arrest (Monastrol arrest released into MG132) mostly had closely associated sister chromatids with “closed” or “open” arms (Figure 4B,C**,** Figure 4 – figure supplement 1). By contrast, H3 T118E or H3 T118I caused a higher incidence of chromosomes with “partially separated” arms, indicating loss of arm cohesion and partial loss of centromeric cohesion (Figure 4B,C). Similar defects in cohesion were observed for cells expressing T118E and T118I upon pro-metaphase arrest with the microtubule destabilizing drugs nocodazole and colcemid (data not shown). The loss of cohesion was most pronounced for H3 T118I, where partially separated sister chromatids were predominant in 50% of the cells versus 10% of the cells for wild type H3 (Figure 4C). Furthermore, the proportion of cells where most of the

sister chromatids were totally separated, indicating complete loss of cohesion, was 16% for H3 T118I versus 4% for wild type H3 (Figure 4C). These data indicate that H3 T118E or H3 T118I promotes loss of cohesion at the centromere and chromosome arms. Given the correlation between faulty cohesion and chromosome alignment defects, we propose that the faulty cohesion caused by expression of H3 T118I or T118E is responsible for the defects in chromosome alignment.

Aurora-A overexpression has been linked to aneuploidy and cancer, presumably through its role in centrosome duplication. Aurora-A overexpression has not been linked to cohesion loss previously, but this could provide an alternate explanation for aneuploidy. Therefore, we made isogenic cell lines overexpressing Aurora-A and kinase dead Aurora-A. The cell lines had equal expression of Aurora-A (Figure 4 – figure supplement 2A) and proceeded relatively normally through the cell cycle (data not shown). Overexpression of Aurora-A increased levels of H3 T118ph along the chromosome arms (Figure 4D). We asked if overexpression of Aurora-A recapitulates the loss of cohesion caused by expression of H3 T118I and T118E. Upon colcemid-induced pro-metaphase arrest, overexpression of Aurora-A caused 44% of the sister chromatids to be “partially separated” as compared to 20% for the control cell line (Figure 4E**,** Figure 4 – figure supplement 2B). Because overexpression of Aurora-A leads to cohesion loss, it is likely that cohesion loss in the H3 T118E and T118I mutants is due to their structurally mimicking elevated levels of H3 T118ph.

Excess H3 T118ph leads to defective chromosomal condensation

Because cohesion defects can be caused by altered chromatin integrity, we measured the length and width of chromosome one from each H3 mutant. We identified chromosome one by using a special DAPI-treatment protocol to highlight the large pericentromeric

heterochromatin cluster (Figure 5 – figure supplement 1A). Expression of H3 T118E and T118I made chromosome one significantly wider and shorter (Figure 5A, Figure 5 – figure supplement 1B,C). To investigate centromere integrity in the T118 mutants, we measured the sister chromatid interkinetochore distance in chromosome spreads collected after arrest in metaphase. We found that H3 T118E and T118I significantly increased sister chromatid interkinetochore distances (Figure 5B), as measured by immunostaining for CENP-A (Figure 5 – figure supplement 1D).

To obtain a higher resolution view of the effects of the H3 T118 mutations on chromosome structure, we performed scanning electron microscopy (SEM). Upon pro-metaphase arrest, chromosomes from the H3 wild type and T118A mutant cell lines were organized into loops and coils to form very tight compact structures (Figure 5C). By contrast, mitotic chromosomes from the H3 T118E and T118I cell lines were less tightly packed with longer radiating DNA loops. These results indicate that H3 T118E and T118I disrupt the higher order chromatin packaging. This grossly altered mitotic chromosome structure led us to test whether the H3 T118I mutation causes the histones to be more readily removed from chromatin. In agreement, H3 T118I was more readily extracted from chromatin than wild type H3 at 600mM salt (Figure 5D). Expression of H3 T118I also increased DNA accessibility to the nuclease DNase I in both asynchronous and mitotically arrested cells (Figure 5E, Figure 5 – figure supplement 2A). Together, these results are consistent with biochemical studies that showed that mononucleosomes with H3 T118ph favor the removal of histone H3 from DNA compared to unphosphorylated mononucleosomes (North, Javaid et al. 2011).

Given that overexpression of Aurora-A results in excess H3 T118ph (Figure 4D), we asked if it also disrupts chromosome integrity. Overexpression of Aurora-A caused significant

widening and shortening of the chromosome arms of metaphase chromosomes (Figure 5F) as was observed for H3 T118E and T118I (Figure 5A), while overexpression of Aurora-A KD did not (Figure 5 – figure supplement 2B). Overexpression of Aurora-A also caused increased sister chromatid interkinetochore distances (Figure 5G). These results further indicate that the H3 T118I and T118E mutations are functional mimics of H3 T118 phosphorylation *in vivo*, and show that H3 T118ph disrupts higher order chromatin packaging.

H3 T118I and T118E cause premature removal of cohesin from DNA

The altered chromatin integrity and cohesion defect caused by excess H3 T118ph or mutations that mimic excess H3 T118ph led us to ask whether there was a dissociation of cohesin proteins from DNA due to excess H3 T118ph. During mitotic delay, the intensity of the Rad21/Scc1 component of the cohesion complex along chromosome arms and at centromeres was drastically reduced in cells expressing H3 T118E and T118I (Figure 6A, Figure 6 – figure supplement 1). Mechanistically, the loss of cohesin and the resulting faulty cohesion phenotype that is caused by excess H3 T118ph (Figure 4B,C,E) could result from multiple causes: premature activation of separase, premature removal of cohesion via cohesin phosphorylation, or improper establishment of cohesion. We set out to distinguish amongst these possibilities. To ask if cells expressing H3 T118I and T118E had premature activation of separase during mitotic delay, we analyzed mitotic spreads after incubation with MG132, which prevents degradation of Cyclin B and Securin and therefore inhibits separase activation (Rock, Gramm et al. 1994). The fact that the T118I and T118E mutants still displayed cohesion loss, despite inhibition of separase (Figure 6B), indicates that cohesin loss in the T118E/I mutants is not due to premature separase activity. The bulk of cohesion is removed in pro-metaphase by phosphorylation of the cohesin subunit SA2 by PLK-1 kinase

or Aurora-B kinase (Hauf, Roitinger et al. 2005). We found that the PLK-1 inhibitor, BI2536, and the Aurora-B inhibitor, hesperidin, prevented cohesion loss in all the H3 expressing cell lines (Figure 6B). Sister chromatid cohesion is also facilitated by DNA catenation during DNA replication (Nitiss 2009). To prevent DNA decatenation, we used a specific inhibitor of Topo II, ICRF-193 and found that chromosomes became extremely tangled, indicative that DNA catenation is undisturbed by the H3 T118 mutations (Figure 6B). Taken, together, these data indicate the H3 T118I and T118E mutations do not disrupt the proper establishment of sister chromatid cohesion by both DNA and sister chromatid catenation, but are likely to lead to premature cohesion loss via the PLK-1 or Aurora-B mediated pathway.

Premature loss of condensin I from DNA due to H3 T118E, T118I and overexpression of Aurora-A

During our PLK-1 inhibition studies, we observed that chromosomes from cells expressing H3 T118I were extremely short (Figure 7A, Figure 7 – figure supplement 1A), a phenotype observed previously (van Vugt, Bras et al. 2004). These short chromosomes occurred in 90% of the mitotic spreads from PLK-1 inhibited cells expressing H3 T118I compared to 22% for wild type H3. This hypercondensation phenotype suggests that H3 T118I may cause disrupt chromosome scaffolding proteins involved in shaping mitotic chromosomes, including condensin I and II and Topo II. However, H3 T118ph does not co-localize with Topo II (Figure 7 – figure supplement 1B) or condensin I (Figure 7B). Next, we determined whether the amounts of the scaffold proteins condensin I, condensin II and Topo II were altered on mitotic chromosomes in the H3 T118 mutants. The staining of Topo II (Figure 7 – figure supplement 2A,B) and condensin II (Figure 7 – figure supplement 3A,B) was similar among cells expressing wild type or mutant H3. However upon mitotic delay, by the error correction assay, there was a significant loss of turbo-GFP (tGFP) tagged condensin I CAP-H protein in

375 both H3 T118E (25% of mitotic cells were tGFP negative) and T118I (50% of mitotic cells
376 were tGFP negative) cell lines as compared to wild type H3 (0% of mitotic cells were GFP
377 negative) (Figure 7C,D). These data demonstrate that H3 T118I and T118E results in
378 reduced levels of condensin I, but not condensin II or Topo II, on chromatin, suggesting that
379 H3 T118ph plays a role in reducing condensin I occupancy on the chromatin.
380
381 Given that mutations that mimic H3 T118ph had reduced condensin I occupancy, we asked
382 whether H3 T118ph directly prevents the binding of condensin I to chromatin. We purified the
383 condensin I complex (Figure 7 – figure supplement 4A) and used expressed protein ligation
384 to generate mononucleosomes that were 100% phosphorylated on H3 T118 (North, Javaid et
385 al. 2011). The histones carrying H3 T118ph generated not only canonical nucleosomes, but
386 also altosomes and disomes (Figure 7 – figure supplement 4B) as seen previously (North,
387 Simon et al. 2014). In electrophoretic mobility shift assay (EMSA) at higher levels of
388 condensin 1, we found that condensin I could bind to nucleosomes and the altered histone-
389 DNA forms, irrespective of the phosphorylation status of H3 T118. This result indicates that
390 H3 T118ph does not directly affect condensin I binding to a mononucleosome. As such, we
391 favor the idea that H3 T118ph promotes changes in global chromatin packaging that may
392 indirectly reduce condensin I occupancy. Therefore, we asked if overexpression of Aurora-A
393 recapitulates the loss of condensin I caused by expression of H3 T118I and T118E. Indeed,
394 upon mitotic delay, there was a significant loss of condensin I from chromatin upon Aurora-A
395 overexpression (25% of mitotic cells were GFP negative) as compared to the control (0% of
396 mitotic cells were GFP negative) (Figure 7E). This result shows that excess H3 T118ph leads
397 to condensin I loss from chromatin. Taken together, these data suggest that the function of
398 mitotic H3 T118ph is to indirectly reduce condensin I and cohesin occupancy on chromatin
399 via its influence on chromosome packaging.

Discussion

Here we provide the first *in vivo* characterization of phosphorylation on threonine 118 of histone H3 (H3 T118ph), a modification that breaks histone-DNA contacts at the nucleosomal dyad. In metazoans, H3 T118ph is dynamically regulated through mitosis by the Aurora-A kinase, occurring at pericentromeric regions and at discrete locations on chromosome arms. Excess H3 T118ph (achieved by overexpression of Aurora-A or mimicked by amino acid substitution) resulted in increased numbers of lagging chromosomes, defects in chromosome congression, delayed cytokinesis, altered chromosome compaction, cohesion loss and cohesin and condensin I loss. Normally, H3 T118ph disappears from each chromosome when chromosome alignment is achieved. Given that condensin I increases the rigidity at the centromere (Ribeiro, Gatlin et al. 2009), we propose a model where H3 T118ph alters the chromatin structure to limit condensin I and cohesin occupancy in order to enable efficient attachment to the mitotic spindle and effective chromosome compaction (Figure 8).

Aurora-A is best known for its role in centrosome separation (Dutertre, Descamps et al. 2002). Our data further supports Aurora-A's involvement in chromosome error correction (Chmatal, Yang et al. 2015, Ye, Deretic et al. 2015), specifically through its role in phosphorylating H3 T118 on chromatin. In agreement, the H3 protein sequence K-R-V-T-I fits the R/K/N-R-X-S/T-B consensus site for Aurora-A (where B is a hydrophobic residue) (Ferrari, Marin et al. 2005). We propose that Aurora-A, in partnership with its activator TPX2, is responsible for phosphorylation of H3 T118 on the chromatin arms and centromeres. Fittingly, Aurora-A is detectable at the centromere during mitosis (Chmatal, Yang et al. 2015). Precedent exists for Aurora-A-mediated phosphorylation of centromeric proteins, on

substrates including NDC80 (Ye, Deretic et al. 2015), CENP-A (Kunitoku, Sasayama et al. 2003) and CENP-E (Kim, Holland et al. 2010). In addition to being found at the centromere, H3 T118ph also occurred in a periodic punctuate pattern along the chromosome arms. As such, H3 T118 is the first known target for phosphorylation by Aurora-A along chromosome arms. This raises the question of how Aurora-A/TPX2 is directed to phosphorylate H3 T118 along the chromosome arms. In order to gain insight into this mechanism, we attempted to map exactly where H3 T118ph occurs on chromatin by ChIP-seq, but unfortunately the antisera against H3 T118ph failed in ChIP analysis (data not shown). This was disappointing since we were able to successfully immunoprecipitate H3 T118ph with the antibody (Figure 1F), raising the possibility that the antibody immunoprecipitates only H3 T118ph on free histones. Regardless of how Aurora-A is targeted to chromatin, it is likely that the phosphorylation of H3 T118ph will also require nucleosome disruption by an ATP-dependent nucleosome remodeler given the buried location of this residue within the nucleosome structure. As such, this would provide an additional step to tightly regulate the function of this key histone post-translational modification.

In addition to the insight gained from the location and timing of H3 T118ph, much of our understanding of H3 T118ph function comes from the analysis of histone mutants. Given that we can only express the H3 mutants to be approximately 10% of the total histone H3 in human cells, it is not surprising that the H3 T118A loss of function mutant gave no detectable phenotype in the presence of endogenous H3 T118ph. In contrast, the H3 T118E and T118I mutants clearly had dominant effects on wild type histones in human cells. It should be noted that *Drosophila* cell clones expressing only H3 T118A, H3 T118E, or H3 T118I have significant defects in cell growth (Graves et al., submitted). H3 T118ph acts to physically distort the nucleosomal DNA at the nucleosome dyad in order to loosen the nucleosome

450 structure and generate altered nucleosomal states (North, Simon et al. 2014). Our results
451 show that the alterations to the nucleosome structure that are induced by H3 T118ph impact
452 higher order levels of chromosome packaging. This structural role of phosphorylation of H3
453 T118 can explain why the T118I mutant gave even more drastic phenotypes than T118E in
454 our experiments. Although isoleucine is not the classic phosphomimetic substitution, it does
455 have a large bulky side chain that would distort the trajectory of the nucleosomal DNA around
456 the histone octamer to an even greater extent than the traditional phosphomimetic of glutamic
457 acid. Furthermore, isoleucine mimics the rigidity of phosphate group compared to the flexible
458 side chain of glutamic acid. Functional support for the idea that H3 T118I structurally mimics
459 the effect of phosphorylation of T118 comes from the fact that overexpression of the T118
460 kinase, Aurora-A, leads to identical phenotypes to T118I.
461
462 **H3 T118ph function at the centromere**
463 H3 T118ph appears at pericentromeric regions during prophase and disappears from each
464 chromosome as it aligns at the metaphase plate. Furthermore, the H3 T118I and T118E
465 mutants resulted in displacement of condensin I and cohesin from chromatin and generated
466 chromosomes with looser chromatin packaging. Accordingly, we propose that H3 T118ph
467 plays an important role in organizing the chromatin structure around centromeres to achieve
468 optimal levels of cohesin and condensin I association to permit enough conformational
469 flexibility for microtubule attachment. Condensin I is highly enriched at centromeres in mitosis
470 in metazoans (Kim, Zhang et al. 2013) and promotes the rigidity of the centromere (Gerlich,
471 Hirota et al. 2006). Additionally, Aurora–A has been demonstrated to play a role in error
472 correction by destabilizing microtubule connections of misaligned chromosomes. Upon
473 knockdown or inhibition of Aurora-A the kinetochore, as well as their attachment to
474 microtubules, become more rigid and stable (Chmatal, Yang et al. 2015, Ye, Deretic et al.

2015). As such, H3 T118ph at the centromere appears to act to limit condensin I occupancy in order to increase flexibility at the centromeres of misaligned chromosomes (Figure 8). This idea is supported by chromosomes from cells expressing H3 T118E, T118I or overexpressing Aurora-A having increased interkinetochore distances (Figure 5B,G), which could be indirectly or directly related to the role of H3 T118ph in removal of cohesin and condensin I. However, upon attachment to mitotic spindles from opposite centrosomes, the centromeric regions have to be rigid enough to resist the forces that the microtubules exert on the centromere in order to prevent separation of sister chromatids until anaphase (Musacchio and Salmon 2007). Removal of H3 T118ph as soon as tension is sensed across the kinetochores would allow for better centromere rigidity. Consistent with an important role for H3 T118ph in achieving appropriate microtubule attachment, H3 T118ph remained at centromeres of misaligned chromosomes (Figure 4A).

H3 T118ph function on chromosome arms

H3 T118ph occurs in a punctate periodic pattern along chromosome arms in prophase and pro-metaphase. Excess H3 T118ph (due to overexpression of Aurora-A or mutations that mimic the effect of phosphorylation) leads to gross alterations in chromosome compaction, with wider and shorter chromosome arms and longer, less organized chromatin loops (Figure 5), suggesting that H3 T118ph plays a role in shaping mitotic chromosomes. Mitotic chromosomes have been suggested to be packaged in a two phase process (Naumova, Imakaev et al.). In the first phase, a linear array of chromatin loops form at random, but consistent, positions along the chromosome. In the second phase, the loops longitudinally condense around the axes. These two different phases are mediated by the condensins, where condensin II is required for linear compaction along the chromosome axes while condensin I helps organize chromatin loops around the axes (Shintomi and Hirano 2010,

Green, Kalitsis et al. 2012). Although the timing of appearance of H3 T118ph and condensin I on chromosome arms is similar, their spatial localization along the arms are distinct (Figure 7B). As such, there is no evidence that H3 T118ph physically recruits or displaces condensin I from chromatin. Indeed, other proteins promote condensin recruitment in yeast including kinetochore proteins (Tada, Susumu et al. 2011) and the Ku heterodimer complex, which functions in non-homologous end joining (Tanaka, Tanizawa et al. 2012). Perhaps related to its recruitment mechanism, yeast condensin interacts with histone H2A and H2AZ *in vitro* (Tada, Susumu et al. 2011) and cross-linking mass spectrometry studies have found interactions between condensin I and H2A and H4 (Barysz, Kim et al. 2015). In addition, our evidence indicates that H3 T118 phosphorylation is likely to regulate condensin I occupancy on the chromatin, given that expression of H3 T118I, T118E and overexpression of Aurora-A cause loss of condensin I from chromosome arms (Figure 7C-E). This disruption of condensin I function is in agreement with the longer loops of chromatin that were observed by SEM in the T118E and T118I mutants (Figure 5C). Consistent with the delayed cytokinesis that occurs upon condensin I knockdown (Gerlich, Hirota et al. 2006) the H3 T118I and T118E mutants caused a delay in cytokinesis (Figure 3E). Given that condensin I interacts with chromosomes in a more dynamic manner than condensin II (Gerlich, Hirota et al. 2006),we propose that the dynamic nature of the association of condensin I with chromatin enables H3 T118ph to regulate the levels of condensin I to shape the mitotic chromosomes as they condense. The ratio of condensin I to condensin II is very tightly controlled within cells, given that changes in the ratio profoundly alters the shape of mitotic chromosomes (Shintomi and Hirano 2010, Bakhrebah, Zhang et al. 2015). As such, the removal of H3 T118ph from the chromosome arms by metaphase, either by dephosphorylation or by our preferred model of physical removal of T118 phosphorylated H3 from the DNA, is likely to regulate the ratio of condensin I:condensin II for appropriate chromosome compaction. This

function is likely to occur in an indirect manner via H3 T118ph affecting chromatin structure, given that condensin I binding to mononucleosomes is not affected by H3 T118ph *in vitro* (Figure 7 – figure supplement 4B). Similarly, we propose that the loss of cohesin is an indirect consequence of the altered packaging of the chromatin structure caused by excess H3 T118ph, which may expose the cohesin ring to PLK-1 mediated phosphorylation and subsequent removal of cohesin (Hauf, Roitinger et al. 2005). However, we were unable to rule out the possibility that the cohesion phenotype may be due to loss of Sgo-1-mediated protection against PLK-1 and Aurora-B kinases.

Taken together, our work suggests a model where phosphorylation of H3 T118 at the nucleosome dyad by Aurora-A is a critical step to ensure chromosome congression, via its influence on chromosome compaction and cohesion through physically regulating nucleosome structure. These functions are likely to be conserved in metazoans, as we find similar localization and timing of H3 T118ph in nematodes, flies, and human cells. The importance of the ability to utilize H3 T118ph to alter the nucleosome structure to regulate mitosis is underscored by the embryonic lethality of flies where all of their histones are mutated to prevent T118 phosphorylation or to mimic persistent H3 T118 phosphorylation. Given that Aurora-A is overexpressed in many cancers, it is tempting to speculate that the carcinogenic effect of overexpressed Aurora-A may be mediated at least in part via altering the mitotic chromatin structure by phosphorylation at the nucleosome dyad.

Materials and Methods

Constructs and cloning

Plasmid expressing human H2B:RFP was a kind gift from Walter Hittelman (MDACC). Plasmids expressing human Aurora-A:FLAG and Aurora-A KD:FLAG were a kind gift from Subrata Sen (MDACC) (Katayama, Wang et al. 2012). The CMV-histone *Drosophila* H3-YFP (dH3) plasmid was purchased from Addgene (plasmid 8694). The CapH:GFP plasmid was purchased from Origene (Rockville, MD USA, RG201421). The shRNA histone H3 resistant plasmid pOZ-FH-C H3.1c:FLAG:HA (HuH3.1:FLAG) was kindly provided by Zhenkun Lou (Mayo clinic). Site directed mutagenesis was performed on the CMV-histone dH3-YFP and pOZ-FH-C H3.1c:FLAG:HA plasmids listed below using the QuickChange Site-directed Mutagenesis Kit (Agilent Technologies, Santa Clara, CA, USA 200515). This plasmid has the histone sequence of *Drosophila* histone H3 and corresponds to the human histone H3.2 amino acid sequence. The CMV-histone dH3 YFP T118A plasmid was generated using the following primers:

Forward: 5'- TTCATGCCAAGCGTGTCGCCATAATGCCCAAAGAC -3'

Reverse: 5'- GTCTTTGGGCATTATGGCGACACGCTTGGCATGAA -3'

The CMV-histone dH3 YFP T118E plasmid was generated using the following primers:

Forward:

5'- GCCATTCATGCCAAGCGTGTCGAGATAATGCCCAAAGACATCCAG -3'

Reverse:

5'- CTGGATGTCTTTGGGCATTATCTCGACACGCTTGGCATGAATGGC -3'

The CMV-histone dH3 YFP T118I plasmid was generated using the following primers:

Forward: 5'- TCATGCCAAGCGTGTCATCATAATGCCCAAAGACA -3'

Reverse: 5'-TGTCTTTGGGCATTATGATGACACGCTTGGCATGA -3'

The pOZ-FH-C HuH3.1T118A:FLAG primer was generated using the following primers:

Forward: 5'- CACGCTAAACGCGTCGCCATCATGCCCAAAG -3'

Reverse: 5'- CTTTGGGCATGATGGCGACGCGTTTAGCGTG -3'

The pOZ-FH-C HuH3.1T118E:FLAG plasmid was generated using the following primers:

Forward:

5'- GCTATTCACGCTAAACGCGTCGAGATCATGCCCAAAGATATCCAG -3'

Reverse:

5'- CTGGATATCTTTGGGCATGATCTCGACGCGTTTAGCGTGAATAGC -3'

The pOZ-FH-C HuH3.1T118:FLAG plasmid was generated using the following primers:

Forward: 5'- TCACGCTAAACGCGTCATCATCATGCCCAAAGATA -3'

Reverse: 5'- TATCTTTGGGCATGATGATGACGCGTTTAGCGTGA -3'

The following primers were used for a PCR ligation reaction to amplify HuH3.1:FLAG

Forward: 5'-ATGGCTCGTACGAAGCAAAC-3'

Reverse: 5'-CTAGGCGTAGTCGGGCACGTCGT -3'

The resulting PCR fragment was cloned into pcDNA5 FRT/TO TOPO TA plasmid (Life technology Grand Island, NY USA K6510-20)

Antibodies and peptides

Mad2 antibody was a kind gift from Ted Salmon (UNC, Chapel Hill). The following primary antibodies were purchased: polyclonal H3 T118ph (Abcam Cambridge, MA USA ab33310, lot 7 for western blots and lot 9 for immunofluorescence), H3S10ph (Abcam, ab14955), C-terminal H3 (Abcam, ab1791), N-terminal H3 (Active Motif Carlsbad, CA USA, 39763), γ-tubulin (Abcam, ab27074), CENP-A (Abcam, ab8245), CENP-A (Cell Signal Boston, MA

599 USA, 2186), GAPDH (Abcam, ab8245), M2-FLAG (Sigma St. Louis, MO USA, F3165),
600 BubR1 (Abcam, ab4637), Hec1 (Abcam, ab3613), CENP-E (Abcam, ab4163), Hp1α (Active
601 Motif, 39295), HP1β (Active Motif, 39979) HP1γ (Active Motif, 39981), Aurora-B/AIM-1 (BD
602 Biosciences, 611082), SA2 (Bethyl laboratories, Montgomery, TX USA, A310-043A), Rad21
603 (Millipore Billerica MA, USA 05-908), H3 K9 me3 (Abcam, ab6001), CapD3 (Bethyl
604 laboratories, A300-604A), Topo II (Milllipore, MAB4197), (phospho) Aurora-A T288 (Cell
605 Signaling, 3079), Aurora-A Clone 35C1 (Invitrogen, 45-8900), α-tubulin (Sigma-Aldrich,
606 T9026), α-tubulin (AbD Sterotec Raleigh, NC, USA MCA78G), anti-GFP (Roche Indianapolis,
607 IN USA 11814460001), and anti-turboGFP (Origene TA150041).
608 The secondary antibodies used were as follows: Alexa Fluor® 488 goat anti-rabbit (Life
609 Technologies, A11034), Alexa Fluor® 594 goat anti-rabbit (A11037), Alexa Fluor® 488 goat
610 anti-mouse (A11029), Alexa Fluor® 555 goat anti-rat (Cell Signaling, Danvers, MA, USA),
611 HRP-conjugated anti-mouse (Promega, Madison, WI USA, PR-W4011), and HRP-conjugated
612 anti-rabbit (PRW4021).
613 Non-biotinylated peptides used were H3 unmodified (Abcam, ab12149), H3 S10ph (Abcam,
614 ab1147), H3 K122ac (Abcam, ab34466), and H3 T118ph (Abcam, ab33505). Biotinylated
615 peptides were either purchased from Anaspec (Freemont, CA, USA) or were a kind gift from
616 Min Gyu Lee (MDACC).
617
618 **Cell lines and stable cell lines**
619 HeLa cells were maintained in Dulbecco's Modified Eagle Medium (DMEM) supplemented
620 with 10% fetal bovine serum and 1% penicillin/streptomycin. WI-38 cells were maintained in
621 Eagle's Minimum Essential Medium (MEM) supplemented with 10% fetal bovine serum and
622 1% penicillin/streptomycin. MCF10A cells were maintained in DMEM/Nutrient Mixture F-12

supplemented with 5% horse serum, 1% penicillin/streptomycin, 10 mg/ml insulin, 1 mg/ml hydrocortisone, 25 µg/ml EGF, and 1 mg/ml cholera toxin. The Flp-in T-Rex 293 (293TR) cell line was purchased from Life Technologies (R780-07) and were maintained in DMEM 10% fetal bovine serum and 1% penicillin/streptomycin.

Stable cell lines of HuH3.1 FLAG:HA were made by transfecting 293TR cells with 1µg of pcdna5 FRT huH3.1FLAG:HA, and 9ug of POG44 (Life Technologies, V6005-20), using the Nucleofector kit according to the manufacturers instructions (Lonza Basel Switzerland, V4XC-2012). One day post transfection, cells were washed with fresh medium. Two days post transfection polyclonal stable cell lines were selected by maintaining cells in 400µg/ml hygromycin. Stable cell lines expressing Aurora-A:FLAG, Aurora-A KD:FLAG and CapH:tGFP were made by transfecting 293TR cells (and desired H3 mutant cell lines) with 1µg of plasmid, using lipofectamine 2000 according to the manufacturer's instructions. Two days post-transfection, stable cell lines were selected by maintaining cells in media containing 800 µg/ml G418.

Tissue culture siRNA transfection

Cells were plated in a six-well dish and were grown to 50% to 60% confluence. For siRNA inhibition studies, the cells were co-transfected with 0.5µg plasmid pBos H2B:RFP and siGENOME Human AURKA siRNA (Thermo Scientific Lafayette, CO USA, D-003545-05-0005) or ON-TARGET plus non-targeting siRNA #1 (Thermo Scientific, D-001810-01-05) (at a final concentration of 100 nM) in the presence of Lipofectamine 2000 reagent (Life Technologies, 11668019), as per the manufacturer's instructions. The cells were harvested at 72 hours post transfection for protein extraction and immunofluorescence analysis.

Tissue culture shRNA transfections

For shRNA knockdown studies, three different shRNA constructs (pGipz) were purchased from MD Anderson's shRNA core. The target sequences of TPX2 shRNA are (1) TTAGCAGTGGAATCGAGTG; (2) AACAGGTTAATATCATCCT; (3) ATCTTGATGAGCACTGCCT. Cells were plated in six-well plates with CELL-TAK (BD Biosciences San Jose, CA USA, 354240) were grown to 50% to 60% confluence, and were cotransfected with all three TPX2 target sequences in the presence of Lipofectamine 2000 reagent (Life Technologies, Carlsbad, CA), as per the manufacturer's instructions. After transfection, the cells were split at 72 hours and 1 µg/ml puromycin was added. After 5 days the cells were collected for protein extraction and immunofluorescence analysis.

***C. elegans* and RNAi mediated interference**

Wild type N2 Bristol *C. elegans* were grown and maintained at 20°C as described (Brenner 1974). The feeding method of RNAi delivery was used to deplete CENP-A/HCP-3, as previously described by Timmons and Fire (Timmons and Fire 1998). RNAi plasmids for CENP-A/*hcp-3* were obtained from the Geneservice Ltd. *C. elegans* feeding library (Kamath and Ahringer 2003). *E. coli* HT115 (DE3) bacteria was transformed with the control or CENP-A/HCP-3 RNAi plasmids. 1 ml LB + 100 µg/µl ampicillin liquid culture was inoculated with a single colony of HT115 bacterial transformation and grown overnight at 37°C. The following day these cultures were expanded into 50 ml LB/amp using a 1:100 dilution and grown for six hours at 37°C. After six hours, 200 µl were spread onto single nematode growth (NG) plates supplemented with 20% β-lactose and placed at 25°C for 72 hours. Subsequently, the plates

were seeded with L4-stage hermaphrodites and incubated at 25°C for 24 hours (Arur, Ohmachi et al. 2009). The L4440 RNAi vector was used as an RNAi control.

Chromosome attachment error correction assay and drug treatments

We used an Eg5 inhibitor, Monastrol, to induce a monopolar spindle and kinetochore-microtubule attachment errors (Sanhaji, Friel et al. 2010). For the chromosome attachment error correction assays (monastrol-release experiments), cells were split into a 6 well dish at least 24 hours prior to treatment. Cells at 75% confluency were treated for 4 hrs with monastrol (100 µM, Enzo Life Sciences, Farmingdale NY USA, BML-GR322-0005) and washed and released into fresh medium containing MG132 (20 µM, Calbiochem, Billerica, MA USA, 474790-1MG, in ETOH) for 2hrs and cells collected for immunofluorescence. All inhibitors were used at the listed concentrations MG132 (20 µM in ETOH), RO-3306 (9 µM, Enzo Life Sciences, ALX-270-463-M001,in DMSO), Nocodazole (100 mg/ml, Sigma, M1404, in ETOH), Colcemid (0.01 µg/mL, Roche 10295892001), PLK-1 inhibitor BI-2536 (100 nM, Selleck chemicals , Houston, TX USA, S1109, in DMSO), Caffeine (80 nM, Sigma C0750, in DMEM), Aurora-B inhibitor ZM447439 (2µM, Tocris Biosciences, S1103, in DMSO), Calyculin A (50 nM, Tocris Biosciences, in EtOH), Aurora-B inhibitor Hesperidin (1 µM Selleck chemicals S2309, in DMSO), Aurora-A inhibitor VX-680 (1µM, Selleck chemicals, S1048, in DMSO), Aurora-A inhibitor MLN 8237 (1 µM, Selleck Chem, S1133, in DMSO), Topoisomerase II inhibitor ICRF 193 (10µM, Sigma, U4659, in DMSO).

Tissue culture immunofluorescence

Immunofluorescence of metaphase chromosome spreads was prepared by cytospin following the pre-extraction method as described previously (Ono, Losada et al. 2003). Immunofluorescence of adherent cells were grown on poly-D-lysine coated coverslips (BD

Biosciences, 354086) and harvested prior to reaching 80% confluency. Coverslips were washed in 1× PBS and fixed in 4% paraformaldehyde/1 x PBS for 10 min at room temperature (Electron Microscopy Sciences Hatfield, PA USA, 15710). Coverslips were washed in 1 x PBS and then permeabilized with 1 x PBS + 0.1% Triton X-100 at RT for 10mins. Coverslips were then washed in 1 x PBS and blocked in 3% BSA/1× PBS for 1 h. Primary antibodies were diluted into 3% BSA/1 x PBS and incubated overnight at 4 ºC. Coverslips were washed 3 times 1× PBS for 15 minutes prior to adding secondary antibodies. Coverslips were washed 3 times in 1 x PBS for 15 minutes and mounted onto glass slides with ProLong® Gold Antifade mounting reagent containing DAPI (Life Technologies, Grand Island, NY, USA, Cat# P36931). Immunofluorescence images were acquired as described below.

***C. elegans* immunostaining**

Embryos from adult hermaphrodites were picked into 10 µl egg buffer on a Poly-L-Lysine coated glass slide (Sigma, St Louis, MO P0425). To release the embryos, a coverslip was placed over the animals and gentle pressure was applied. The slides were subsequently placed on an aluminum plate over dry ice for 1 hour. To crack the embryo's cuticle and aid its permeabilization, coverslips were quickly snapped off. Slides were fixed in -20°C methanol for 20 minutes, followed by sequential rehydrations: 80:20, 50:50, and 20:80 methanol to 1x PBS with 0.1% Tween (PBST). After hydration, samples were blocked in 1X PBST with 1% BSA for 1 hour at room temperature and then incubated overnight in primary antibody diluted in PBST at 4°C. Primary antibodies used were anti-tubulin (1:2000, Sigma), and H3 T118ph (1:1000). Samples were then washed with PBST and secondary antibodies were applied for 2 hours at room temperature. Secondary antibodies used were: Alexa Fluor 488 goat anti-mouse IgG and Alexa Fluor 594 goat anti-rabbit (both at 1:1000) (Invitrogen Molecular

720 Probes, Eugene, OR). After incubation with the secondary antibodies the samples were
721 washed with PBST and mounted using ProLong® Gold Antifade ProLong with DAPI.
722 Immunofluorescence images were acquired as described below.
723
724 **Mitotic chromosome spreads**
725 Cells were collected by mitotic shake off. Media was removed and the cells were pelleted at
726 1000 rpm for 5 mins. All but 1 ml of media was removed and gently used to resuspend cells.
727 Cells were swollen in 10 ml of hypotonic solution (46.5 mM KCl/8.5 mM NaCitrate) and
728 incubated for 20 mins at 37°C. Fresh Carnoy's fixative (3:1 methanol:acetic acid) was added
729 to hypotonic buffer at 10% (v/v). Subsequent to centrifugation cells, were fixed 3 times with
730 10 mls Carnoy's fixative for 10 mins at RT followed by pelleting the cells at 1000 rpm for 5
731 mins. Pellets were than resuspended in a small volume of Carnoy's fixative, dropped onto
732 positively charged slides (Fisher scientific, Ashville, NC USA,12-550-15) air-dried, and
733 stained with 1 mg/ml DAPI solution diluted 1:15,000. Slides were mounted with ProLong®
734 Gold Antifade mounting reagent containing DAPI. Immunofluorescence images were
735 acquired as described below. To stain heterochromain, chromosome spreads were treated as
736 in (Hirota, Gerlich et al. 2004) except 0.08 mg/ml netropsin was used instead of distamycin.
737
738 **SEM**
739 We followed published methods (Lai, Wong et al. 2011). Chromosome spreads were
740 prepared as described above except the chromosomes were dropped onto poly-D-lysine
741 coated coverslips (BD Biocoat, 354086) in a 37°C room with minimal drying. The coverslips
742 were flipped onto a larger coverslip with 1 drop of 45% acetic acid and the large coverslip
743 was placed on dry ice for 15 mins. The chromosome spreads were then fixed in 2.5%
744 glutaraldehyde / 1 x PBS overnight at 4°C. The fixed samples were than washed with distilled

745 water for 5 min, 10 min, and 15 min, then dehydrated with a graded series of increasing
746 concentrations of ethanol (5 mins in 70%, 10 min in 90% and 15 min in 100%). The samples
747 were then chemically dried in a graded series of increasing concentrations of
748 hexamethyldisilazane (HMDS, Electron Microscopy Services) 2:1 (100% EtOH:HMDS), 1:1
749 (100% EtOH: 100% HMDS), then 1:2 (100% EtOH: HMDS), then 3 changes in pure HMDS
750 where all steps were for 5 mins each. Then the samples were air dried overnight. Samples
751 were mounted onto an aluminum specimen mount (Ted pella, INC.) by carbon conductive
752 double-stick tape (Ted Pella. Inc., Redding, CA). The samples were then coated under
753 vacuum using a sputter system (208HR, Cressington Scientific Instruments, England) with
754 platinum alloy for a thickness of 30 nm. Samples were examined in a Nova NanoSEM 230
755 scanning electron microscope (FEI, Hillsboro, Oregon) at an accelerating voltage of 10 kV.
756
757 **Indirect immunofluorescence of chromosome spreads**
758 In general, to produce chromosome spreads, HeLa mitotic cells obtained by mitotic shake off
759 were incubated in pre-warmed hypotonic buffer (46.5 mM KCl/8.5 mM NaCitrate) at 37°C for
760 8–10 min. 293TR mitotic cells obtained by selective detachment were incubated in pre-
761 warmed hypotonic buffer #5 (10 mM Tris-HCl pH7.4, 40 mM glycerol, 20 mM NaCl, 1.0 mM
762 $CaCl_2$, 0.5 mM $MgCl_2$). After attachment to Poly-D-lysine glass coverslips by Cytospin at
763 1000 rpm for 2 min, chromosome spreads were pre-extracted with 0.1% Triton X-100/1 x
764 PBS for 2 mins and were than fixed with 2% PFA/1 x PBS at RT for 10 min. Cells were
765 extracted with 0.1% Triton X-100/PBS for 10 mins. Blocking occurred in 1 x PBS, 3% BSA,
766 and 0.1% Triton X-100, for 30 min at room temperature. Once blocking was complete, the
767 immunofluorescence protocol was followed as described above.
768
769

Extended chromatin fibers

Cells were arrested with colcemid and the chromatin fibers were generated as described elsewhere (Dunleavy, Almouzni et al. 2011). Briefly, chromatin fibers from human cells were prepared by incubating 6-8x10^4 cell/ml in prewarmed hypotonic buffer at 37°C for 10 mins. HeLa cells used hypotonic buffer 46.5 mM KCl/8.5 mM Na Citrate and for 293TR used the buffer was 10 mM Tris-HCl pH 7.4, 40 mM glycerol, 20 mM NaCl, 1.0 mM $CaCl_2$, 0.5 mM $MgCl_2$. Cells were centrifuged onto charged microscope slides (Fisher Scientific, 2-550-15) and lysed for 14min in salt detergent buffer supplemented with urea (10 mM Tris HCl pH 7.5, 1% Triton X-100, 500 mM NaCl, and 500 mM urea) before slowly aspirating the lysis buffer by vacuum and fixing in 2% PFA/1 x PBS. Slides were incubated in 1× PBST (1× PBS + 0.1% Triton X-100) and blocked in 1 x PBS, 1% BSA, 0.1% Triton X-100, for 30 min at room temperature. Once blocking was complete, the immunofluorescence protocol was followed as described above.

Isolation of pellet and supernatant fractions

Two D150 plates, at 80% confluency, were collected by mitotic shake off. Cells were pelleted and washed in TB buffer (20 mM Hepes, pH 7.3, 110 nM K-acetate, 5 mM Na-acetate, 2 mM Mg-acetate, 1 mM EGTA, 2 mM DTT, and a protease inhibitor cocktail (Roche, Complete-mini, cat#1187350001). All steps were done at 4°C. NP40 extraction of detergent soluble proteins was performed by treatment with 0.1% NP40 for 5 mins, followed by centrifugation at 3000 rpm for 3 mins to separate the non-chromatin supernatant and chromatin pellet fractions. The pellet fractions were subsequently digested with 20 µg/ml DNaseI (Worthington Biochemical Corporation, Lakewood, NJ USA, LS006342) for 10 mins at 37°C. Total, supernatant (non-chromatin), and pellet (chromatin) fractions were resolved by SDS-PAGE and analyzed by western blotting.

795

796 **Differential salt solubility**

797 The method was adapted from (Henikoff, Henikoff et al. 2009) with the differences detailed
798 below. Five million cells were pelleted during the nuclei extraction on ice samples and were
799 divided into 5 tubes. The Nuclei were washed in NIM buffer (0.25 M sucrose, 25 mM KCl, 5
800 mM $MgCl_2$, 10 mM Tris-HCL pH 7.4). Pelleted at 300rpm for 5 mins. The nuclei were
801 resuspened in 5 different extraction buffers at increasing salt concentration (0, 600, 900,
802 1200, and 1500 mM NaCl) Incubated on ice for 10 mins. The soluble and pellet fractions
803 were collected by centrifugation at 13,000 rpm for 10 mins. 5xSDS was added to the soluble
804 fractions and boiled at 100°C for 5 mins. The pellet fractions were resuspended in 250µl
805 Laemmli buffer and the Whole Cell Extract protocol was followed (as detailed below).

806

807 **Whole cell extracts**

808 Approximately 2×10^6 cells were lysed with 200 µl Laemmli buffer (4% SDS, 20% glycerol,
809 and 120 mM Tris pH 6.8). Cells were subsequently vortexed for 30 secs and then boiled at
810 100 °C for 5 min. After briefly cooling, samples were vortexed for 30 secs and sonicated for
811 10 secs at 20% power. Lastly, 5 x SDS buffer was added to samples to obtain a 1x final
812 concentration and samples were boiled at 100°C for 5 min.

813

814 **Immunoprecipitation**

815 Whole cell extracts were prepared using RIPA buffer (150 mM NaCl, 1% NP40, 0.5% sodium
816 deoxycholate, 0.1% SDS, 50 mM Tris, pH 8, 10 mM NaF, 0.4 mM EDTA, 10% glycerol and
817 protease inhibitors) supplemented with 10x phostop (Roche 04906845001), and 25x
818 Protease inhibitor (Roche 04693132001). The pre-blocked protein-A–Dynabeads (Thermo-

819 Fischer, 10001D) was then incubated with whole-cell extracts overnight in 4°C. The antibody
820 was added for 4hours the next day. Following extensive washes, the bead-bound protein
821 complexes were analyzed by western blotting using H3 C-term antibody.
822
823 **Western blot analysis**
824 Samples were resolved by 15% SDS-PAGE and transferred to nitrocellulose according to
825 standard procedures. For HRP detection, following transfer the membranes were blocked in
826 5% non-fat milk (w/v) in 1× TBST for 1 hr. The blots were probed with primary antibodies at
827 room temperature for 1 h or overnight at 4ºC. Blots were washed and incubated in secondary
828 antibodies at room temperature for 1 hr. ECL detection was either by Amersham ECL
829 Western Blotting Detection Reagents (GE, Pittsburgh, PA USA, RPN2106) or Immobilon
830 Western Chemiluminescent HRP Substrate (Millipore, WBKLS0500). Alpha viewer was used
831 to analyze and quantitate bands (Proteinsimple, Santa Clara, CA, USA). For LICOR
832 Odyssey detection the transfer blots were blocked in Sea Block buffer (Thermo Scientific,
833 Cat#37527) in 1 x PBS for 1 hr. Blots were incubated with primary and secondary antibodies
834 as described above. An Odyssey imager was used to analyze and quantitate bands.
835
836 **Peptide dot blots**
837 Lyophilized peptides were rehydrated in 1 x PBS at a 10 µM concentration. The peptides
838 were serially diluted to the indicated concentrations and dotted out onto activated PVDF
839 membrane. The membrane was air-dried and then stained with amido black to verify the
840 presence of the peptides. The membranes were washed in PBS and then blocked in 3%
841 BSA/1 x PBS. The blots were incubated in primary antibodies overnight at 4 ºC. The blots

were washed and probed with HRP conjugated secondary antibodies at room temperature for 1 hr. Alpha viewer was used to analyze and quantitate bands (Proteinsimple).

Peptide competition assay

Biotinylated peptides (4 µg total) were incubated with 400 µl H3 T118ph antibody for 45 min at room temperature (RT). Samples were centrifuged for 15 min at 4 ºC at 13 k rpm. 300 µl of each supernatant was used for indirect immunofluorescence as described above.

DNase 1 fragmentation assay

Approximately 2×10^6 cells were lysed with 2 mL of lysis buffer (50 mM Tris-HCl pH 7.9, 100 mM KCl, 5 mM MgCl2, 0.05% v/v saponin, 50% v/v glycerol, 0.5M DTT, 10x phostop (Roche 04906845001), and 25x Protease inhibitor (Roche 04693132001) of asynchronous or synchronized cells (synchronized for 6hrs in nocodazole (100mg/ml, in ETOH)). Cells were incubated in lysis buffer for 3 minutes on ice and vortexed every minute. Samples were centrifuged for 10 min at 4 ºC at 1000 x g. Nuclei were subsequently digested for increasing times at 37°C with 5U DNase I (Worthington Biochemical Corporation LS006342) in TB buffer (20 mM Hepes, pH 7.3, 110 nM Potassium-acetate, 5 mM Sodium-acetate, 2 mM Magnesium-acetate, 1mM EGTA, 2 mM DTT and a protease inhibitor cocktail (Roche, Complete-mini, cat#1187350001)). Fragmented DNA was purified and analyzed by agarose gel electrophoresis followed by Sybr Gold (Life Technologies, S-11494) staining for visualization with a FluorChem E FE05000 (Protein simple, San Jose, CA). Plot profiles were obtained with ImageJ software.

Live cell imaging

A four well chamber was coated with BD Bio TAK according to the manufacturer's instructions. Approximately 24 hours prior to live cell imaging, HEK293 cells were transfected using the Nucleofector kit according to the manufacturers instructions (Lonza,V4XC-2012) with 0.5 µg plasmid CMV:H3.2 YFP wild type or T118 mutant. The transfected cells were plated at 50,000 cells per well and grown in a humidified chamber for 24 hrs. At the time of imaging, the cells were placed in a prewarmed Oko Full Enclosure incubator at 37°C with 5% CO_2. Cells were imaged using a 3i Marianas Spinning Disk Confocal equipped with an Evolve 10 MHz Digital Monochrome Camera (Photometrics, Tuscon, AZ USA) and images were taken every 5 mins for 16 hours and driven by Slidebook 5.5 software (a 63 x 1.49 NA Plan Apo oil immersion objective). Three Z-sections were acquired for each cell. The start of cytokinesis was defined when H3:YFP chromatin decondensed after anaphase. The end of cytokinesis was determined by the physical separation of the cytoplasmic membrane.

Acquisition of images

The majority of images were acquired on a 3i Marianas Spinning Disk Confocal equipped with a coolSNAP HQ2 CCD Camera. Slidebook 5.5 software was used with a 63 x 1.49NA Plan Apo oil immersion objective and Z sections were acquired at 0.2 um steps. Intensity measurements were calculated with Slidebook 5.5 software. To measure inter-kinetochore distance, the center intensity of foci was determined by Imaris Bitplane software.
Some immunofluorescence images were acquired on a Nikon 2000U inverted microscope equipped with a Photometrics Coolsnap HQ camera. Metamorph software was used with a 60x 1.49NA Plan Apo oil immersion objective and Z sections were acquired at 0.2µm steps.

EMSA

Histone octamers unmodified and modified at H3T118ph were purified according to the method North et. al. (North, Javaid et al. 2011). The Condensin I complex was purified from 5 x 10^6 CAP-H-GFP-SBP, SMC2-SBP and GFP-SBP mitotic cells using the method by Kim et. al. (Kim, Chang et al. 2010). After purification, proteins were eluted in SEB (50 mM Tris pH7.4, 250 mM NaCl, 0.5% NP-40, 0.1% Deoxycholate and 4 mM Biotin). 10 ml samples were subjected to NuPAGE SDS-PAGE and protein and evaluated by silver staining. The EMSA was performed as described previously (Kimura, Kotani et al. 1997).

Generation of flies with H3 T118 mutations

The following genotypes were used in this study:

yw; Df(2L)His^{C}/ CyO, P{ActGFP}JMR1; 6xHisGU^{VK33,27}/ TM6B

yw; Df(2L)His^{C}/ CyO, P{ActGFP}JMR1; 6xHisGU ^{VK33,27} H3T118A/ TM6B

yw; Df(2L)His^{C}/ CyO, P{ActGFP}JMR1; 6xHisGU ^{VK33,27} H3T118E/ TM6B

yw; Df(2L)His^{C}/ CyO, P{ActGFP}JMR1; 6xHisGU ^{VK33,27} H3T118I/ TM6B

We constructed *6xHisGU ^{VK33,27}* and *6xHisGU ^{VK33,27} H3T118A, E* and *I* chromosomes essentially as previously described (Gunesdogan, Jackle et al. 2010) with the following changes: ΦC31attB3xHisGU.H3T118A, ΦC31attB3xHisGU.H3T118E, and ΦC31attB3xHisGU.H3T118I plasmids (further referred to collectively as H3T118A/E/I) were generated by replacing the EcoR1/Sac1 fragment in pENTR221-HisGU with a synthetic fragment (Integrated DNA Technologies, Inc., Iowa, USA) containing an ACC into GCC codon exchange leading to the H3 T118A mutation, an ACC into GAG codon exchange leading to the H3 T118E mutation, or an ACC into AUC codon exchange leading to the H3 T118I mutation. The pENTRL4R1-HisGU.H3T118A/E/I and pENTRR2L3-HisGU.H3T118A/E/I entry vectors were generated by moving the Acc65I/AgeI fragment from

915 the pENTR221-HisGU.H3T118A/E/I mutant vectors to the pENTRL4R1 and the pENTRR2L3
916 vectors. Recombination of pENTR221-HisGU.H3T118A/E/I, pENTRL4R1-
917 HisGU.H3T118A/E/I and pENTRR2L3-HisGU.H3T118A/E/I with pDESTR3R4-ΦC31attB
918 resulted in the ΦC31attB3xHisGU.H3T118A/E/I transgenic constructs. We utilized ΦC31-
919 mediated transgenesis to integrate these constructs, as well as ΦC31attB3xHisGU, site
920 specifically into the *Drosophila* genome using the landing sites *VK27* and *VK33* (Venken, He
921 et al. 2006). Homozygous viable insertions from each site were recombined to generate
922 *6xHisGU* ^{VK33,27} and *6xHisGU* ^{VK33,27} *H3T118A, E* and *I* chromosomes and crossed into the
923 *Df(2L)His*^{C} mutant background (Gunesdogan, Jackle et al. 2010). *Df(2L)His*^{C} was kept
924 heterozygous over *CyO, P{ActGFP}JMR1 to* identify mutant embryos lacking green
925 fluorescent protein expression, and the viability of *12xHisGU* transgene containing mutant
926 and wild type animals was assessed. Wild type controls were either non-mutant sibling
927 embryos (internal control) or embryos which contain *12xHisGU* (WT control), which both
928 survive to adult viability.
929
930
931 **Acknowledgments**
932 We acknowledge Ted Salmon for providing antibodies and Walter Hittelman, Sen Subrata,
933 and Zhenkun Lou for plasmids. We are grateful to Rick Fishel for discussions at the early
934 stages of this project. We thank Henry Adams for his assistance with microscopy and
935 analysis. We thank Alf Herzig for the plasmids and fly stocks. We are grateful to Hugo Bellen,
936 Yuchun He and Hongling Pan for *Drosophila* embryo injections. We thank Alan J. Tackett and
937 Stephanie Byrum for mass-spec analyses, Kenneth Dunner Jr for help with the SEM, Jinhua
938 Gu (SEM/AFM core at Houston Methodist Hospital Research Institute) for assistance. We
939 thank Ngoc H. Bui for technical assistance and Jason Ford, Jessica Orbeta, and Tokiko

Furuta for help with *C. elegans* experiments. We thank Brandee Price and Ja-Hwan Seol for comments on the manuscript. We thank Brad Cairns for his support during the review process. This work was supported by NIH grant GM64475.

References

Arur, S., M. Ohmachi, S. Nayak, M. Hayes, A. Miranda, A. Hay, A. Golden and T. Schedl (2009). "Multiple ERK substrates execute single biological processes in Caenorhabditis elegans germ-line development." Proceedings of the National Academy of Sciences of the United States of America **106**(12): 4776-4781.

Bakhrebah, M., T. Zhang, J. R. Mann, P. Kalitsis and D. F. Hudson (2015). "Disruption of a conserved CAP-D3 threonine alters condensin loading on mitotic chromosomes leading to chromosome hyper-condensation." J Biol Chem.

Barysz, H., J. H. Kim, Z. A. Chen, D. F. Hudson, J. Rappsilber, D. L. Gerloff and W. C. Earnshaw (2015). "Three-dimensional topology of the SMC2/SMC4 subcomplex from chicken condensin I revealed by cross-linking and molecular modelling." Open Biol **5**(2): 150005.

Brenner, S. (1974). "The genetics of Caenorhabditis elegans." Genetics **77**(1): 71-94.

Cosgrove, M. S., J. D. Boeke and C. Wolberger (2004). "Regulated nucleosome mobility and the histone code." Nat Struct Mol Biol **11**(11): 1037-1043.

963 Crosio, C., G. M. Fimia, R. Loury, M. Kimura, Y. Okano, H. Zhou, S. Sen, C. D. Allis and P.
964 Sassone-Corsi (2002). "Mitotic phosphorylation of histone H3: spatio-temporal regulation by
965 mammalian Aurora kinases." Mol Cell Biol **22**(3): 874-885.
966 Dunleavy, E. M., G. Almouzni and G. H. Karpen (2011). "H3.3 is deposited at centromeres in
967 S phase as a placeholder for newly assembled CENP-A in G(1) phase." Nucleus **2**(2): 146-
968 157.
969 Ferrari, S., O. Marin, M. A. Pagano, F. Meggio, D. Hess, M. El-Shemerly, A. Krystyniak and
970 L. A. Pinna (2005). "Aurora-A site specificity: a study with synthetic peptide substrates."
971 Biochem J **390**(Pt 1): 293-302.
972 Ganem, N. J. and D. Pellman (2012). "Linking abnormal mitosis to the acquisition of DNA
973 damage." J Cell Biol **199**(6): 871-881.
974 Gerlich, D., T. Hirota, B. Koch, J. M. Peters and J. Ellenberg (2006). "Condensin I stabilizes
975 chromosomes mechanically through a dynamic interaction in live cells." Curr Biol **16**(4): 333-
976 344.
977 Green, L. C., P. Kalitsis, T. M. Chang, M. Cipetic, J. H. Kim, O. Marshall, L. Turnbull, C. B.
978 Whitchurch, P. Vagnarelli, K. Samejima, W. C. Earnshaw, K. H. Choo and D. F. Hudson
979 (2012). "Contrasting roles of condensin I and condensin II in mitotic chromosome formation."
980 J Cell Sci **125**(Pt 6): 1591-1604.
981 Gunesdogan, U., H. Jackle and A. Herzig (2010). "A genetic system to assess in vivo the
982 functions of histones and histone modifications in higher eukaryotes." EMBO Rep **11**(10):
983 772-776.
984 Hauf, S., E. Roitinger, B. Koch, C. M. Dittrich, K. Mechtler and J. M. Peters (2005).
985 "Dissociation of cohesin from chromosome arms and loss of arm cohesion during early
986 mitosis depends on phosphorylation of SA2." PLoS Biol **3**(3): e69.

Hirota, T., D. Gerlich, B. Koch, J. Ellenberg and J. M. Peters (2004). "Distinct functions of condensin I and II in mitotic chromosome assembly." J Cell Sci **117**(Pt 26): 6435-6445.

Kamath, R. S. and J. Ahringer (2003). "Genome-wide RNAi screening in Caenorhabditis elegans." Methods **30**(4): 313-321.

Katayama, H., J. Wang, W. Treekitkarnmongkol, H. Kawai, K. Sasai, H. Zhang, H. Wang, H. P. Adams, S. Jiang, S. N. Chakraborty, F. Suzuki, R. B. Arlinghaus, J. Liu, J. A. Mobley, W. E. Grizzle, H. Wang and S. Sen (2012). "Aurora kinase-A inactivates DNA damage-induced apoptosis and spindle assembly checkpoint response functions of p73." Cancer Cell **21**(2): 196-211.

Katsuki, Y., S. Nakada, T. Yokoyama, I. Imoto, J. Inazawa, M. Nagasawa and S. Mizutani (2008). "Caffeine yields aneuploidy through asymmetrical cell division caused by misalignment of chromosomes." Cancer Sci **99**(8): 1539-1545.

Kim, J. H., T. M. Chang, A. N. Graham, K. H. Choo, P. Kalitsis and D. F. Hudson (2010). "Streptavidin-Binding Peptide (SBP)-tagged SMC2 allows single-step affinity fluorescence, blotting or purification of the condensin complex." BMC Biochem **11**: 50.

Kim, J. H., T. Zhang, N. C. Wong, N. Davidson, J. Maksimovic, A. Oshlack, W. C. Earnshaw, P. Kalitsis and D. F. Hudson (2013). "Condensin I associates with structural and gene regulatory regions in vertebrate chromosomes." Nat Commun **4**: 2537.

Kim, Y., A. J. Holland, W. Lan and D. W. Cleveland (2010). "Aurora kinases and protein phosphatase 1 mediate chromosome congression through regulation of CENP-E." Cell **142**(3): 444-455.

Kimura, M., S. Kotani, T. Hattori, N. Sumi, T. Yoshioka, K. Todokoro and Y. Okano (1997). "Cell cycle-dependent expression and spindle pole localization of a novel human protein kinase, Aik, related to Aurora of Drosophila and yeast Ipl1." J Biol Chem **272**(21): 13766-13771.

Kornberg, R. D. (1974). "Chromatin structure: a repeating unit of histones and DNA." Science **184**(4139): 868-871.

Kruger, W., C. L. Peterson, A. Sil, C. Coburn, G. Arents, E. N. Moudrianakis and I. Herskowitz (1995). "Amino acid substitutions in the structured domains of histones H3 and H4 partially relieve the requirement of the yeast SWI/SNF complex for transcription." Genes Dev **9**(22): 2770-2779.

Kufer, T. A., H. H. Sillje, R. Korner, O. J. Gruss, P. Meraldi and E. A. Nigg (2002). "Human TPX2 is required for targeting Aurora-A kinase to the spindle." J Cell Biol **158**(4): 617-623.

Kunitoku, N., T. Sasayama, T. Marumoto, D. Zhang, S. Honda, O. Kobayashi, K. Hatakeyama, Y. Ushio, H. Saya and T. Hirota (2003). "CENP-A phosphorylation by Aurora-A in prophase is required for enrichment of Aurora-B at inner centromeres and for kinetochore function." Dev Cell **5**(6): 853-864.

Lai, S. K., C. H. Wong, Y. P. Lee and H. Y. Li (2011). "Caspase-3-mediated degradation of condensin Cap-H regulates mitotic cell death." Cell Death Differ **18**(6): 996-1004.

Lee, J., T. S. Kitajima, Y. Tanno, K. Yoshida, T. Morita, T. Miyano, M. Miyake and Y. Watanabe (2008). "Unified mode of centromeric protection by shugoshin in mammalian oocytes and somatic cells." Nat Cell Biol **10**(1): 42-52.

Mersfelder, E. L. and M. R. Parthun (2006). "The tale beyond the tail: histone core domain modifications and the regulation of chromatin structure." Nucleic Acids Res **34**(9): 2653-2662.

Musacchio, A. and E. D. Salmon (2007). "The spindle-assembly checkpoint in space and time." Nat Rev Mol Cell Biol **8**(5): 379-393.

Muthurajan, U. M., Y. Bao, L. J. Forsberg, R. S. Edayathumangalam, P. N. Dyer, C. L. White and K. Luger (2004). "Crystal structures of histone Sin mutant nucleosomes reveal altered protein-DNA interactions." EMBO J **23**(2): 260-271.

1036 Naumova, N., M. Imakaev, G. Fudenberg, Y. Zhan, B. R. Lajoie, L. A. Mirny and J. Dekker
1037 "Organization of the mitotic chromosome." Science **342**(6161): 948-953.
1038 Nitiss, J. L. (2009). "DNA topoisomerase II and its growing repertoire of biological functions."
1039 Nat Rev Cancer **9**(5): 327-337.
1040 Nonaka, N., T. Kitajima, S. Yokobayashi, G. Xiao, M. Yamamoto, S. I. Grewal and Y.
1041 Watanabe (2002). "Recruitment of cohesin to heterochromatic regions by Swi6/HP1 in fission
1042 yeast." Nat Cell Biol **4**(1): 89-93.
1043 North, J. A., S. Javaid, M. B. Ferdinand, N. Chatterjee, J. W. Picking, M. Shoffner, R. J.
1044 Nakkula, B. Bartholomew, J. J. Ottesen, R. Fishel and M. G. Poirier (2011). "Phosphorylation
1045 of histone H3(T118) alters nucleosome dynamics and remodeling." Nucleic Acids Res **39**(15):
1046 6465-6474.
1047 North, J. A., M. Simon, M. B. Ferdinand, M. A. Shoffner, J. W. Picking, C. J. Howard, A. M.
1048 Mooney, J. van Noort, M. G. Poirier and J. J. Ottesen (2014). "Histone H3 phosphorylation
1049 near the nucleosome dyad alters chromatin structure." Nucleic Acids Res **42**(8): 4922-4933.
1050 Olsen, J. V., M. Vermeulen, A. Santamaria, C. Kumar, M. L. Miller, L. J. Jensen, F. Gnad, J.
1051 Cox, T. S. Jensen, E. A. Nigg, S. Brunak and M. Mann (2010). "Quantitative
1052 phosphoproteomics reveals widespread full phosphorylation site occupancy during mitosis."
1053 Sci Signal **3**(104): ra3.
1054 Ono, T., A. Losada, M. Hirano, M. P. Myers, A. F. Neuwald and T. Hirano (2003). "Differential
1055 contributions of condensin I and condensin II to mitotic chromosome architecture in
1056 vertebrate cells." Cell **115**(1): 109-121.
1057 Polioudaki, H., Y. Markaki, N. Kourmouli, G. Dialynas, P. A. Theodoropoulos, P. B. Singh and
1058 S. D. Georgatos (2004). "Mitotic phosphorylation of histone H3 at threonine 3." FEBS Lett
1059 **560**(1-3): 39-44.

Ribeiro, S. A., J. C. Gatlin, Y. Dong, A. Joglekar, L. Cameron, D. F. Hudson, C. J. Farr, B. F. McEwen, E. D. Salmon, W. C. Earnshaw and P. Vagnarelli (2009). "Condensin regulates the stiffness of vertebrate centromeres." Mol Biol Cell **20**(9): 2371-2380.

Rock, K. L., C. Gramm, L. Rothstein, K. Clark, R. Stein, L. Dick, D. Hwang and A. L. Goldberg (1994). "Inhibitors of the proteasome block the degradation of most cell proteins and the generation of peptides presented on MHC class I molecules." Cell **78**(5): 761-771.

Sanhaji, M., C. T. Friel, N. N. Kreis, A. Kramer, C. Martin, J. Howard, K. Strebhardt and J. Yuan (2010). "Functional and spatial regulation of mitotic centromere-associated kinesin by cyclin-dependent kinase 1." Mol Cell Biol **30**(11): 2594-2607.

Shintomi, K. and T. Hirano (2010). "Sister chromatid resolution: a cohesin releasing network and beyond." Chromosoma **119**(5): 459-467.

Strahl, B. D. and C. D. Allis (2000). "The language of covalent histone modifications." Nature **403**(6765): 41-45.

Tada, K., H. Susumu, T. Sakuno and Y. Watanabe (2011). "Condensin association with histone H2A shapes mitotic chromosomes." Nature **474**(7352): 477-483.

Tanaka, A., H. Tanizawa, S. Sriswasdi, O. Iwasaki, A. G. Chatterjee, D. W. Speicher, H. L. Levin, E. Noguchi and K. Noma (2012). "Epigenetic regulation of condensin-mediated genome organization during the cell cycle and upon DNA damage through histone H3 lysine 56 acetylation." Mol Cell **48**(4): 532-546.

Thompson, S. L. and D. A. Compton (2011). "Chromosome missegregation in human cells arises through specific types of kinetochore-microtubule attachment errors." Proc Natl Acad Sci U S A **108**(44): 17974-17978.

Timmons, L. and A. Fire (1998). "Specific interference by ingested dsRNA." Nature **395**(6705): 854.

van Vugt, M. A., A. Bras and R. H. Medema (2004). "Polo-like kinase-1 controls recovery from a G2 DNA damage-induced arrest in mammalian cells." Mol Cell **15**(5): 799-811.

Venken, K. J., Y. He, R. A. Hoskins and H. J. Bellen (2006). "P[acman]: a BAC transgenic platform for targeted insertion of large DNA fragments in D. melanogaster." Science **314**(5806): 1747-1751.

Zeitlin, S. G., R. D. Shelby and K. F. Sullivan (2001). "CENP-A is phosphorylated by Aurora B kinase and plays an unexpected role in completion of cytokinesis." J Cell Biol **155**(7): 1147-1157.

Figure Legends

Figure 1. Dynamic mitotic phosphorylation of H3 T118. A. The side chain of H3 T118 (red) is close enough to form a hydrogen bond with the DNA (grey). Histone H3 is depicted in dark blue, Histone H4 is cyan, Histone H2A is green and H2B is yellow. Angstrom distances were drawn using nearest neighbor wizard in pymol. Protein Data Bank (PDB) code 1KX5. **B**. The indicated amounts of the respective peptides were dotted and the membrane probed with an antibody to histone H3 T118ph. The UnM T118 peptide corresponds to human histone H3 aa 115 to 125. **C.** Western blot of crude extract from HeLa cells, using infra-red labeled secondary antibodies. H3 T118ph (greyscale/red) and N-term histone H3 (green) **D.** HeLa cell extracts untreated or treated with phosphatase inhibitor were probed with the indicated antibodies. Full western blot image can be found in Fig. 1-S1A. **E**. HeLa cells were synchronized by a double thymidine arrest and released at the indicated times, followed by western blot analysis of whole cell extracts. **F**. Immunoprecipitation (IP) using the H3 T118ph antibody from HeLa cells asynchronous (Asynch) or released from a G_2 arrest (with 9μM Ro-3306 for 16hrs) for 30 mins resulting in pro-metaphase cells (Pro-M). Full western blot image can be found in Fig. 1-S1B. **G**. Immunofluorescence analysis of H3 T118ph (green) and α-tubulin (red) in HeLa cells. Scale bar = 10 μm. **H**. H3 T118ph antibody was pre-incubated with no peptide (top), H3 phosphorylated at T118 (middle) or unmodified (UnM T118, bottom). The supernatants were used to detect H3 T118ph in pro-metaphase HeLa cells. Scale bar = 10 μm.

Figure 2. H3 T118ph localizes to pericentromeres and chromosome arms during prophase and pro-metaphase. A. Immunofluorescence of two-cell *C. elegans* embryos Control (RNAi) (top) and centromeric protein A CENP-A (RNAi)-depleted (bottom) embryos were fixed and stained with α-tubulin (green) and H3 T118ph (red) antibodies. DNA was

stained with DAPI (blue). Scale bar = 5 μm. **B-E.** Immunofluorescence of HeLa cells stained with CENP-A (red) and H3 T118ph (green) antibodies. **B.** Images of progressive mitotic stages. **C**. Mitotic spreads synchronized with colcemid (no tension across the kinetochores). The white box indicates magnified area. Intensity of the signal across centromeres is plotted. Scale bar = 5 μm. **D**. Unsynchronized mitotic spread, as in C. **E**. Extended metaphase chromatid fibers showing H3 T118ph localization to discrete regions of chromosome arms.

Figure 3. Aurora-A phosphorylates H3 T118 and mutations that mimic T118 phosphorylation cause mitotic defects. A. *In vitro* kinase activity of Aurora-A,-B,-C for H3 T118 peptide. **B**. Immunofluorescence of pro-metaphase HeLa cells cotransfected with H2B:RFP and siRNA to Aurora-A (bottom) or control scrambled siRNA (top). Scale bar = 5 μm. **C**. Cytokinesis in 293TR cells transiently transfected with H3-YFP plasmids. YFP (yellow) and DNA stained with DAPI (blue). Scale bar = 5 μm. **D**. Quantitation of C (n=30 cells in anaphase, ** p=0.01, by Fishers exact test). Error bars represent SD of the mean (SDM). **E**. Quantitative data of live cell imaging showing differences in average length in cytokinesis during live cell imaging (n = 50 cells, ** $p<0.01$ and *** $p<0.001$ by unpaired student t-test). **F**. Error correction assay for 293TR stable cell lines expressing H3. Inhibition of Aurora-B with ZM447439 represents an extreme case of inability to correct error. Scale bar =10 μm **G**. Quantitation of cells with misaligned chromosomes on the metaphase plate as in F. (* $p<0.05$ and *** $p<0.001$ by Fishers exact test). Error bars represent SDM.

Figure 4. H3 T118I, T118E and Aurora-A overexpression lead to premature loss of cohesion. A. Immunofluorescence of HeLa cells representing pro-metaphase (top panel), metaphase (middle panel) and caffeine-treated (bottom). The primary antibodies used were histone H3 T118ph (green), BubR1 (red) and DNA was stained with DAPI (blue). Scale bar =

5 μm. **B**. Chromosome spreads of H3 T118 mutant cell lines following the error correction assay either untreated (left) or monastrol (middle) then released into MG132 (right). Scale bar = 5 μm. **C**. The degree of cohesion loss for Monastrol (-) and Monastrol washout MG132 (+) treatments were scored from B. (n=100 cells per treatment collected over 3 experiments, ** $p<0.01$ and *** $p<0.001$ by unpaired student t-test). Error bars represent the SDM **D**. Chromosome spreads of 293TR cell lines with over expression of Aurora-A or Aurora-A KD. The primary antibodies used were against CENP-A (magenta), H3 T118ph (green), and DNA was stained with DAPI (blue). Scale bar = 5 μm. **E**. Quantitation of Fig. S4C colcemid pro-metaphase arrest (Pro-M). (n=100 cells per treatment, collected over 3 experiments *** $p<0.001$ by unpaired student t-test). Error bars represent the SDM.

Figure 5. Altered chromosomal compaction due to H3 T118E, H3 T118I or overexpressing Aurora-A. **A**. Measurement of the width and length of chromosome one for over 50 chromatids for each H3 WT:FLAG and H3 T118I:FLAG stable cell lines (*** $p<0.001$ by Wilcoxon rank sum test). **B**. Interkinetochore distances for pairs of sister chromatids. N=100 centromeres from 5 mitotic chromosome spreads (* = $p<0.01$ by student t-test). Error bars represent SD of the mean (SDM). **C**. SEM images taken at 50K and 100K magnification upon prolonged mitotic arrest. Scale bar = 1 μm. **D.** Western analysis of soluble (free histones) and pellet (chromatin) fractions following successive increasing concentration NaCl extractions. **E.** Dnase-I digestion analysis on nocodazole arrested cells. Densitometric profiles are shown on the right. **F.** As in A, comparing 293TR versus Aurora–A overexpressing cell lines for over 30 chromatids (*** $p<0.001$ and ** $p<0.01$ by Wilcoxon rank sum test). **G.** As in B, comparing 293TR cell lines with over expression of Aurora-A or Aurora-A KD with and without colcemid arrest (Pro-M arrest, pro-metaphase arrest). N=50

centromeres from 5 mitotic spreads (*** = p<0.001 by student t-test). Error bars represent SDM.

Figure 6. Premature cohesion loss in the phosphomimetic and SIN mutants is independent of separase activity, but dependent on proper centromere tension. A. Mitotic spreads following the error correction assay. The primary antibodies used were against Rad21, cohesion subunit (magenta), CENP-A (green), and DNA was stained with DAPI (blue). Scale bar = 5 μm. **B**. Quantitation of the degree of cohesion loss for H3:FLAG stable cell lines, upon proteasome inhibition with MG132, treatment with colcemid, Aurora-B (hesperidin), Plk-1 (BI-2536), and Topo-II (ICRF-193) inhibitors for 3 hr was scored (n=75 cells, per treatment collected over 3 experiments). Insets show representative chromosomes for each type of defect: closed, open, partially separated, separated or tangled.

Figure 7. Reduced condensin I association with chromatin due to H3 T118E and T118I **A.** Chromosome spreads upon PLK-1 inhibition and quantitation of the degree of cohesion loss for H3: WT:FLAG and H3 T118I:FLAG stable cell line. Insets show representative chromosomes for each type of defect: closed and short. (n=50 cells). Scale bar = 5 μm. **B.** Extended chromatin fibers from 293TR CAP-H:tGFP cells. Scale bar = 2 μm. The primary antibodies used were against tGFP (green), H3 T118ph (red), and DNA was stained with DAPI (blue). **C.** Representative mitotic spreads for condensin I (CAP-H:tGFP) positive and tGFP negative cell. The primary antibodies used were against tGFP (green), CENP-A (red), and DNA was stained with DAPI (blue). Scale bar = 5 μm. **D.** Quantitation of number of cells with positive condensin I (CAP-H:tGFP) for mutant H3 stable cell lines treatment without Monastrol (-) and Monastrol washout followed by MG132 (+) treatments. SDM is for three independent experiments (n=100 per treatment). **E.** As in **D**, quantitation using 293TR and

1207 Aurora-A overexpressing cell line from over 50 mitotic spreads in each condition. Error bars
1208 are SDM.
1209
1210 **Figure 8. Model for the functions of H3 T118ph** as explained in the text.
1211
1212 **Supplementary Figure Legends**
1213
1214 **Figure 1 – figure supplement 1. Full size western blots of data shown in Fig. 1. A.** Full
1215 image of western blot probed with H3 T118ph from Fig. 1D. **B**. Full image of
1216 immunoprecipitation analysis western blot probed with antibody to histone H3 for Fig. 1F.
1217 labels are abbreviated the same as in Fig 1F. The "*" marks the non-specific IgG band.
1218
1219 **Figure 3 – figure supplement 1. Results of in vitro kinase screen on peptide spanning**
1220 **H3 T118.** Kinase screen was performed by ProQinase. Kinase activity values (in cpm,
1221 corrected for peptide background) of 190 Ser/Thr kinases performed with 1μM biotinylated
1222 peptide containing amino acids 112 to 123 of H3. The Y-axis set to zero.
1223
1224 **Figure 3 – figure supplement 2. A. Aurora-A inhibitors lead to decreased H3 T118ph.**
1225 Asynchronous HeLa cells were treated with or without Mln8237 or Vx680 and immunostained
1226 with antibodies to H3 T118ph (green), and CENP-A (red) and DNA was stained with DAPI
1227 (blue). Representative pro-metaphase cells are shown. Scale bar = 5 μm. **B. Test of**
1228 **efficiency of the Aurora-A knockdown for experiments shown in Fig. 3 onwards.** Whole
1229 cell extracts were resolved by SDS-PAGE and analyzed by western blot with antibodies to
1230 Aurora-A and GAPDH. Quantitation of Aurora-A protein levels normalized to GAPDH. Shown
1231 is the average and standard deviation from three independent experiments.

Figure 3 – figure supplement 3. A. Control for showing that Aurora-A knockdown worked to decrease phosphorylation of a known substrate. HeLa cells were cotransfected with H2B:RFP and siRNA to Aurora-A or control scrambled siRNA. Coverslips were collected 72 hrs post transfection and immunostained with primary antibody Aurora-A T288ph (green). Scale bar = 5 μm. **B. Knockdown of TPX2 leads to reduced H3 T118ph.** HeLa cells were cotransfected with H2B:RFP and siRNA to Aurora-A or control scrambled siRNA. Coverslips were collected 72 hrs post transfection and immunostained with primary antibody Aurora-A T288ph (green). Scale bar = 5 μm. **C. Knockdown of TPX2 reduces Aurora-A activity in pro-metaphase.** Knockdown was performed as in B. Representative images of immunostained with primary antibody to Aurora-A T288ph (red) are shown. Scale bars = 5 μm.

Figure 3 – figure supplement 4. A. Consistent level of expression of YFP tagged wild type and mutant H3. Western blot analysis of whole cell extract from transient transfections following live cell imaging of H3 WT:YFP and H3:YFP mutants. The blot was probed with a GFP specific antibody. Histone H3 and GAPDH are shown as loading controls. **B. Time spent in mitosis is not significantly affected by expression of H3 or T118 mutants.** Quantitation of the duration pro-metaphase to an anaphase of transiently transfected H3.2:YFP, H3.2 T118E:YFP, and H3.2 T118I:YFP taken from analysis of live cell imaging of YFP. The average and standard deviation of three independent experiments is shown. **C. Time spent in mitosis is not significantly affected by addition of H3 or T118 mutants.** Quantitative data of live cell imaging of cells progressing through cytokinesis with a lagging chromosome. The average length of cytokinesis for H3:YFP, H3 T118E:YFP, and H3T118I:YFP is marked by the horizontal line. Differences were not statistically significant. **D.**

Equal expression of the FLAG tagged H3 wild type and mutant constructs. Western blot analysis of whole cell extract from 293TR cells stably expressing wild type and mutant H3:FLAG. The blot was probed for histone H3 to detect endogenous H3 and H3:FLAG. GAPDH is shown as a loading control. **E. Quantitation of FLAG tagged H3 compared to endogenous H3.** The average and standard deviation of three independent experiments is shown.

Figure 3 – figure supplement 5. A. FLAG-tagged wild type and mutant H3 are equally incorporated into chromatin. Chromatin fractionation following mitotic shake off of 293TR stable cell lines expressing wild type and mutant H3:FLAG. The blot was probed with α-FLAG to detect tagged H3; histone H3 and GAPDH were used as fractionation controls. "Supernatant" contains the soluble proteins while "pellet" contains the insoluble proteins including those on chromatin. **B. Analysis of distribution of cells in different phases of mitosis upon expression of FLAG-tagged wild type and mutant H3.** Stable cell lines of histone H3 WT:FLAG (WT), H3 T118A:FLAG (TA), H3 T118E:FLAG (TE), or H3 T118I:FLAG (TI) were grown on coverslips and arrested in Ro-3306 inhibitor for 24 hrs. Coverslips were collected at the times listed following release into fresh DMEM. At each time point the cells were scored for the phases of the cell cycle phase based on DAPI DNA stain (n=300 mitotic cells for each mutant, per time point, collected over 3 experiments). **C. Expression of wild type and mutant H3 does not make prophase longer.** Quantitation of stable cell lines in pro-metaphase or metaphase upon release from monastrol with arrest in MG132 for 2 hrs (n=75 cells, collected over 3 experiments.

Figure 3 – figure supplement 6. A. Overview of the *Drosophila* system used to replace all H3 with exogenous wild type or mutant H3 expressed from 12 transgenes.

Schematic representation of histone gene organization in *Drosophila melanogaster*. Each histone gene repeat unit contains a single *His1* (red*), His2B (*blue*), His2A (*yellow*), His4* (aqua) and *His3* (purple) gene, which is repeated approximately 100 times on chromosome 2. Transgenes carrying three histone gene units were added one at a time into phiC31 recombination sites on the left and right arms of chromosome 3. This supplies 12 copies of each histone gene to rescue the Δ*HisC* deletion. **B. Stage of development at which lethality occurred due to replace all endogenous H3 with exogenous wild type or mutant H3 expressed from 12 transgenes.**

Figure 4 – figure supplement 1. Metaphase spreads of 293TR stable cell lines expressing wild type H3 or mutant H3 proteins, to demonstrate cohesion defect upon prolonged pro-metaphase arrest. The uncropped images of chromosome spreads in Fig. 4B.The white boxes indicate the magnified image. Scale bar = 5 μm.

Figure 4 – figure supplement 2. A. Demonstration of equivalent expression of exogenous Aurora-A and kinase dead Aurora-A. Total protein extracts from asynchronous and pro-metaphase (Pro-M) mitotically arrested 293TR, Aurora-A:FLAG, and Aurora-A KD:FLAG cells were resolved by SDS-PAGE and analyzed by western blot with antibodies to FLAG, Aurora-A, and GAPDH is used as a loading control. Samples were collected for flow cytometry analysis at the same time. The G_2/M population is listed as a percentage of the mitotic population. **B. Aurora-A overexpression leads to cohesion defects.** Representative chromosome spreads displaying cohesion defects for the control cell lines and overexpressed Aurora-A cell lines untreated (left), arrested with colcemid (right). DNA stained with DAPI (blue). Scale bar = 5 μm. The white boxes indicate the magnified image area. Aurora-A overexpression leads to cohesion defects. After mitotic shake-off to remove

any cells in mitosis, cells were treated with colcemid and chromosome spreads were prepared.

Figure 5 – figure supplement 1. A. Demonstration of how we measured chromosome 1 in metaphase spreads. Representative image of spread chromosomes treated with netropsin followed by DAPI staining. Arrows indicate characteristic heterochromatin of chromosome 1. Dashed lines exemplify the measurements taken of the telomere-to-telomere-length versus the width. Scale bar = 5 μm. **B. Packaging of chromosome 1 is unchanged by T118A.** Chromosome one arm length was measured and plotted against the width of each chromatid for over 50 chromatids (***$p<0.001$ by Wilcoxon rank sum test). **C. Packaging of chromosome 1 is shortened and becomes wider by expression of H3 T118E.** Chromosome one arm length was measured and plotted against the width of each chromatid for over 50 chromatids (***$p<0.001$ by Wilcoxon rank sum test). **D. The interkinetochore distance becomes longer upon expression of T118I.** Representative interkinetochore distances are shown for individual centromeres of each stable cell line marked by CENP-A following a mitotic chromosome spread for asynchronous (left panels) and metaphase arrest (right panel). Scale bar = 1 μm.

Figure 5 – figure supplement 2. A. H3 T118I makes chromatin more accessible to nuclease digestion. Analysis of the Dnase-I digestion products (time 0, 1 min, 2 min, 5 min, 10 min, 20 min) carried out on nuclei isolated from either asynchronous H3 WT:FLAG or H3 T118I:FLAG stable cell lines. Densitometric profiles of each time point of digestion products are shown H3 WT:FLAG (blue) or H3 T118I:FLAG (red). **B. The Aurora-A kinase dead does not change the packaging of chromosome 1, as compared to expression of**

Aurora-A (Figure 5). As in figure 5 – figure supplement B,C. Analysis was of over 30 chromatids for the 293TR versus Aurora-A KD:FLAG stable cell line.

Figure 6 – figure supplement 1. Stable cell lines expressing H3 T118 mutants do not alter Rad21 staining in an asynchronous cell population. Mitotic spreads of an asynchronous cell population from each H3:FLAG stable cell line were subjected to indirect immunofluorescence. The primary antibodies used were Rad21 (magenta), CENP-A (green). DNA was stained with DAPI (blue). The white boxes indicate the magnified image area. Scale bars = 5 μm.

Figure 7 – figure supplement 1. A. PLK-1 inhibition leads to very short chromosomes. The un-cropped images of chromosome spreads in Fig. 7B are shown. The white boxes indicate the magnified image. **B. Topoisomerase II and H3 T118ph display different localization patterns along chromatin fibers.** Extended chromatin fibers were isolated from HeLa cells released for 30 mins from a G_2 arrest. Cells were stained with primary antibodies to H3 T118ph (green) and costained with Topo II (magenta). DNA is stained with DAPI (blue). Scale bar = 5 μm.

Figure 7 – figure supplement 2. A. Topoisomerase II and its levels are unaltered on chromatin from cell lines expressing H3 WT:FLAG, H3 T118A:FLAG, H3 T118E:FLAG and H3 T118I:FLAG. Representative mitotic spreads are shown from asynchronous cultures. The primary antibodies used were against Topo II (magenta), CENP-A (green), and DNA was stained with DAPI (blue). White box indicates magnified image area. Scale bar = 5 μm. **B. Topoisomerase II and its levels are unaltered on chromatin from cell lines**

expressing H3 WT:FLAG, H3 T118A:FLAG, H3 T118E:FLAG and H3 T118I:FLAG upon pro-metaphase arrest. Representative mitotic spreads are shown. The arrest was established via the error correction assay method from each H3:FLAG stable cell line.

Figure 7 – figure supplement 3. A. Condensin II and its levels are unaltered on chromatin from cell lines expressing H3 WT:FLAG, H3 T118A:FLAG, H3 T118E:FLAG and H3 T118I:FLAG in asynchronous cultures. Representative mitotic spreads are shown. The primary antibodies used were CapD3 (condensin II subunit) (magenta) and CENP-A (green). DNA is marked by DAPI (blue). The white boxes indicate the magnified image area. Scale bar = 5 μm. **B. Condensin II and its levels are unaltered on chromatin from cell lines expressing H3 WT:FLAG, H3 T118A:FLAG, H3 T118E:FLAG and H3 T118I:FLAG upon pro-metaphase arrest.** Representative mitotic spreads are shown. The arrest was established via the error correction assay method from each H3:FLAG stable cell line.

Figure 7 – figure supplement 4. A. Purified Condensin I. Silver stain analysis of Streptavidin-Binding Peptide (SBP) tagged SMC2 and CAP-H GFP isolated from chicken DT40 mitotically arrested cells. **B. The binding of Condensin I to nucleosomes is not affected by H3 T118 mutations.** Binding of condensin I to unmodified or H3 T118ph histone octamers reconstituted onto cy5 labeled 247 bp DNA.

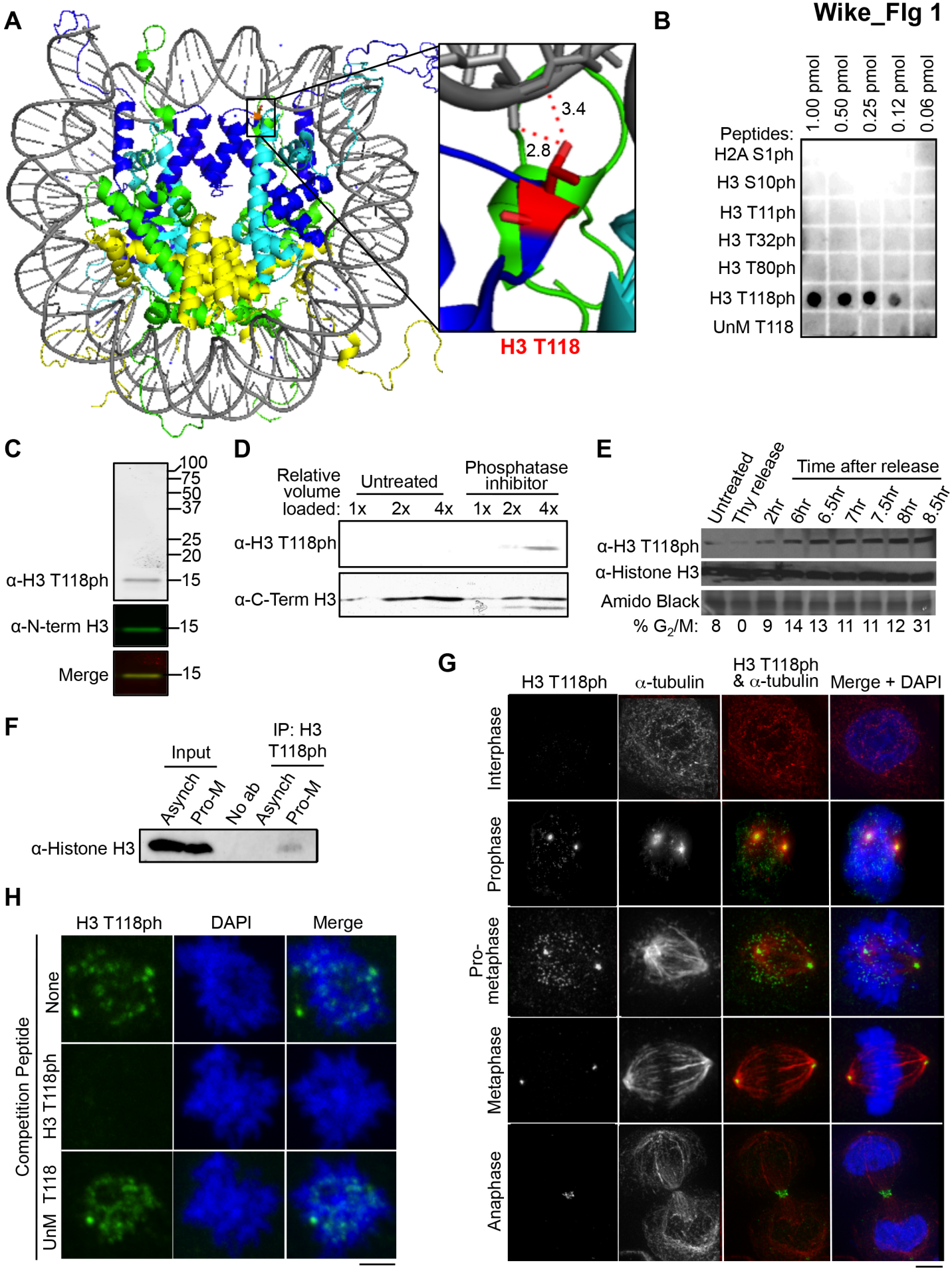
A
3.4
2.8
H3 T118
B
Wike_Flg 1
1.00 pmol
0.50 pmol
0.25 pmol
0.12 pmol
0.06 pmol
Peptides:
H2A S1ph
H3 S10ph
H3 T11ph
H3 T32ph
H3 T80ph
H3 T118ph
UnM T118
C
100
75
50
37
25
20
15
α-H3 T118ph
α-N-term H3
Merge
D
Relative volume loaded:
Untreated
Phosphatase inhibitor
1x 2x 4x 1x 2x 4x
α-H3 T118ph
α-C-Term H3
E
Untreated
Thy release
2hr
Time after release
6hr
6.5hr
7hr
7.5hr
8hr
8.5hr
α-H3 T118ph
α-Histone H3
Amido Black
% G2/M: 8 0 9 14 13 11 11 12 31
F
Input
IP: H3 T118ph
Asynch
Pro-M
No ab
Asynch
Pro-M
α-Histone H3
G
H3 T118ph
α-tubulin
H3 T118ph & α-tubulin
Merge + DAPI
Interphase
Prophase
Pro-metaphase
Metaphase
Anaphase
H
H3 T118ph
DAPI
Merge
Competition Peptide
None
H3 T118ph
UnM T118

Wike_Fig 2

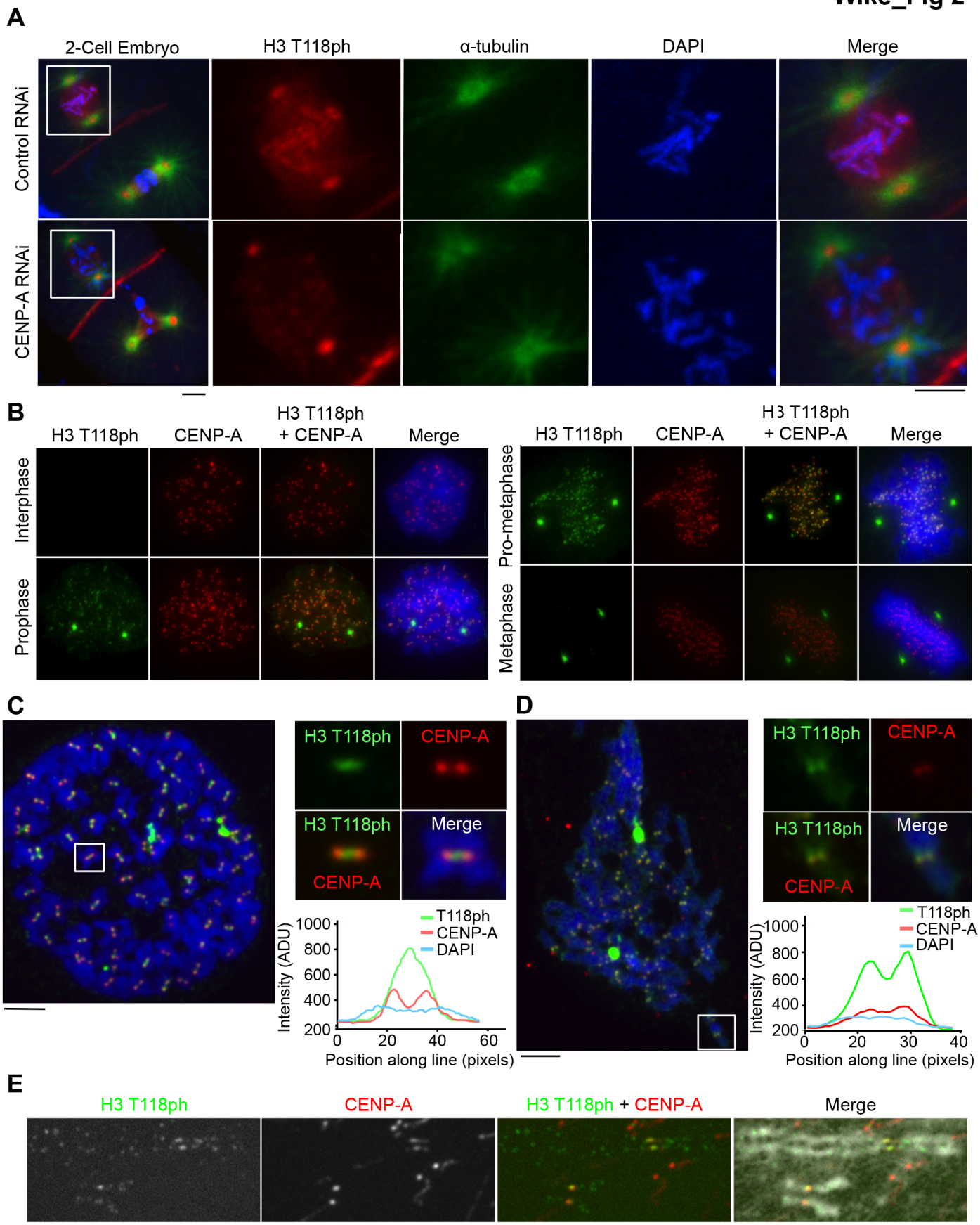
A
2-Cell Embryo
H3 T118ph
α-tubulin
DAPI
Merge
Control RNAi
CENP-A RNAi
B
H3 T118ph
CENP-A
H3 T118ph + CENP-A
Merge
Interphase
Prophase
Pro-metaphase
Metaphase
C
D
H3 T118ph
CENP-A
Merge
T118ph
DAPI
Intensity (ADU)
Position along line (pixels)
E
H3 T118ph + CENP-A

Wike_Fig 3

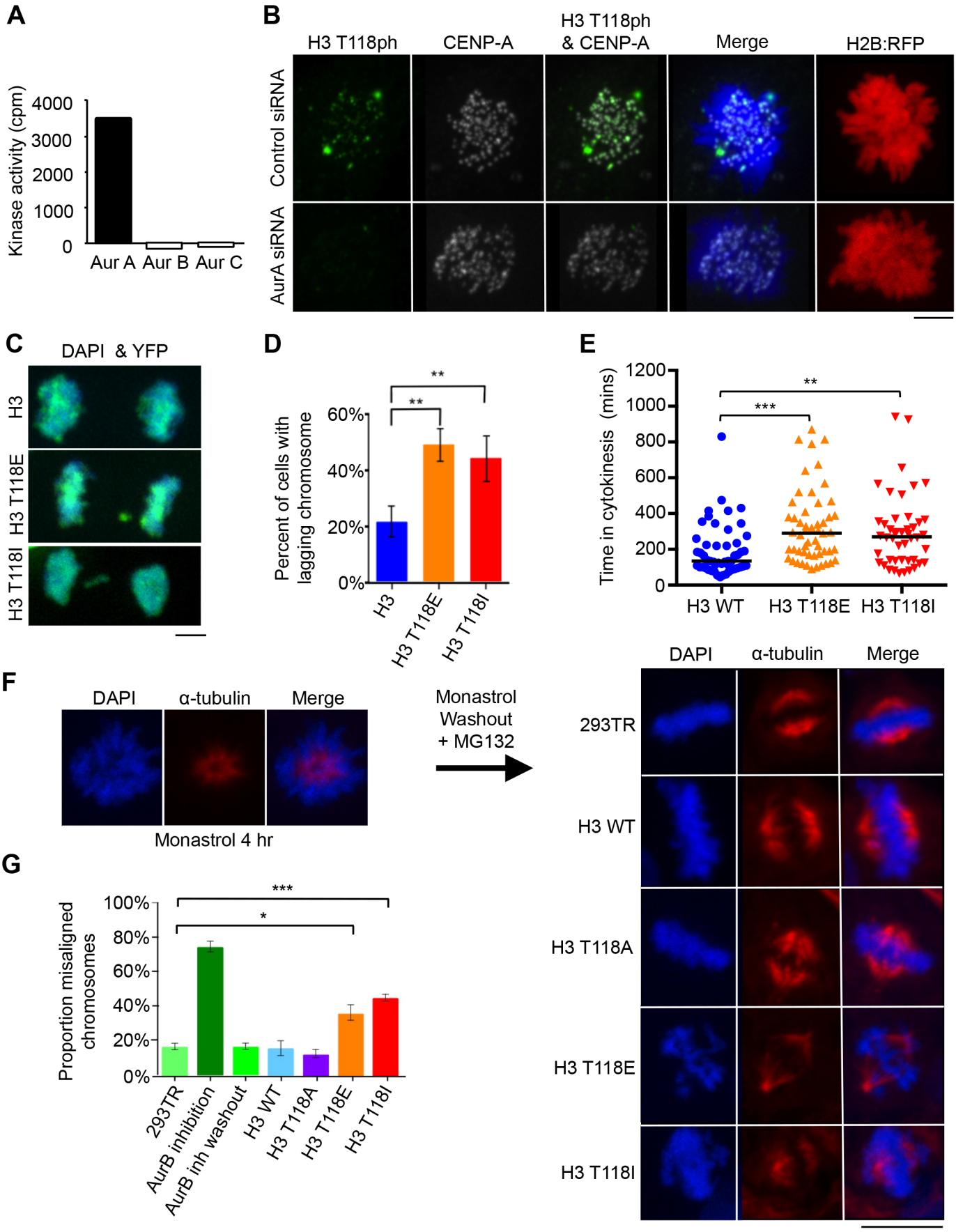
A
Kinase activity (cpm)
4000
3000
2000
1000
0
Aur A
Aur B
Aur C
B
H3 T118ph
CENP-A
H3 T118ph & CENP-A
Merge
H2B:RFP
Control siRNA
AurA siRNA
C
DAPI & YFP
H3
H3 T118E
H3 T118I
D
Percent of cells with lagging chromosome
60%
40%
20%
0%
**
**
H3
H3 T118E
H3 T118I
E
Time in cytokinesis (mins)
1200
1000
800
600
400
200
0
**
***
H3 WT
H3 T118E
H3 T118I
F
DAPI
α-tubulin
Merge
Monastrol 4 hr
Monastrol Washout + MG132
DAPI
α-tubulin
Merge
293TR
H3 WT
H3 T118A
H3 T118E
H3 T118I
G
Proportion misaligned chromosomes
100%
80%
60%
40%
20%
0%
***
*
293TR
AurB inhibition
AurB inh washout
H3 WT
H3 T118A
H3 T118E
H3 T118I

Wike_Fig 4

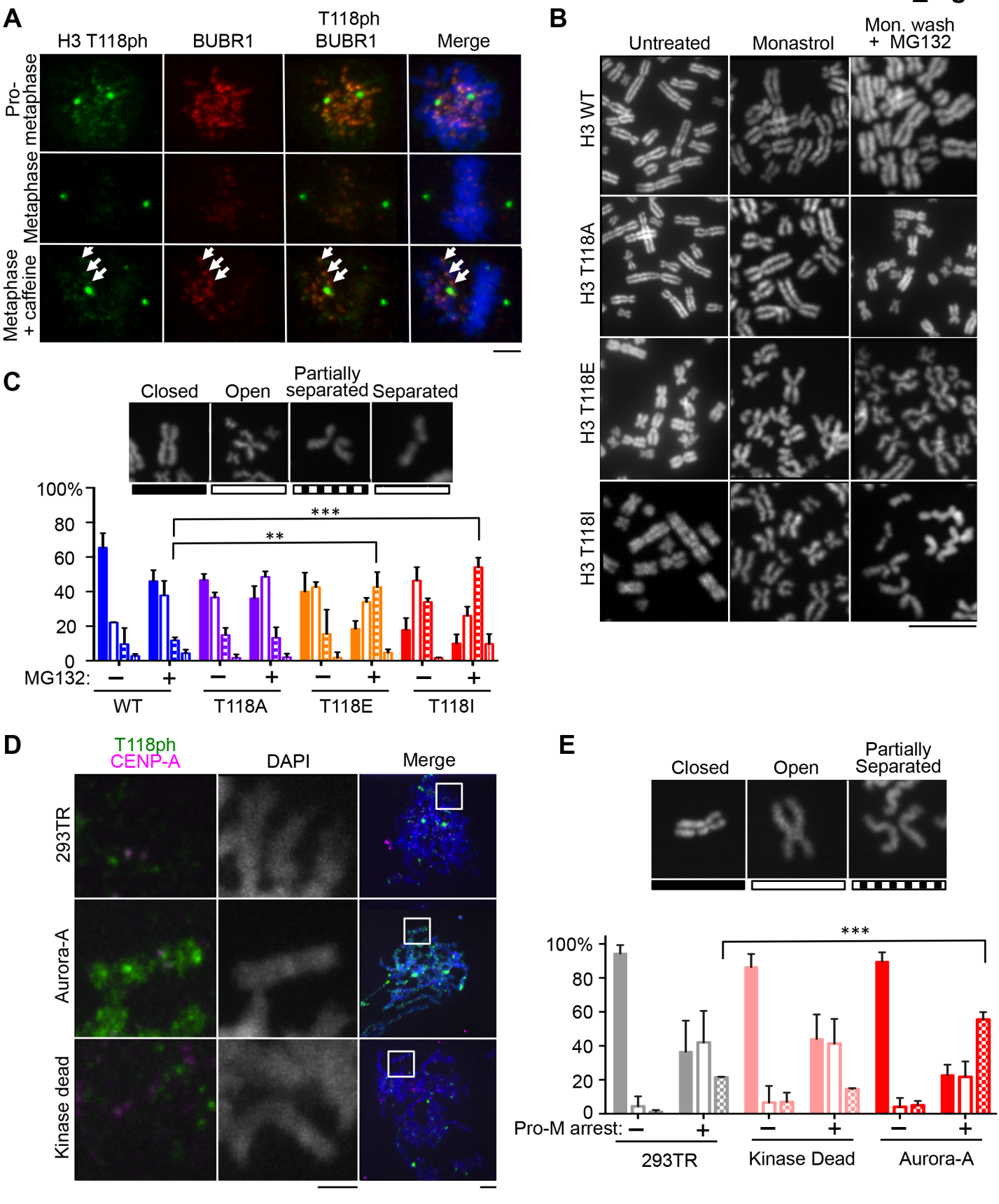
A
H3 T118ph
BUBR1
T118ph BUBR1
Merge
Pro-metaphase
Metaphase
Metaphase + caffeine
B
Untreated
Monastrol
Mon. wash + MG132
H3 WT
H3 T118A
H3 T118E
H3 T118I
C
Closed
Open
Partially separated
Separated
100%
80
60
40
20
0
***
**
MG132:
WT
T118A
T118E
T118I
D
T118ph
CENP-A
DAPI
Merge
293TR
Aurora-A
Kinase dead
E
Closed
Open
Partially Separated
100%
80
60
40
20
0
***
Pro-M arrest:
293TR
Kinase Dead
Aurora-A

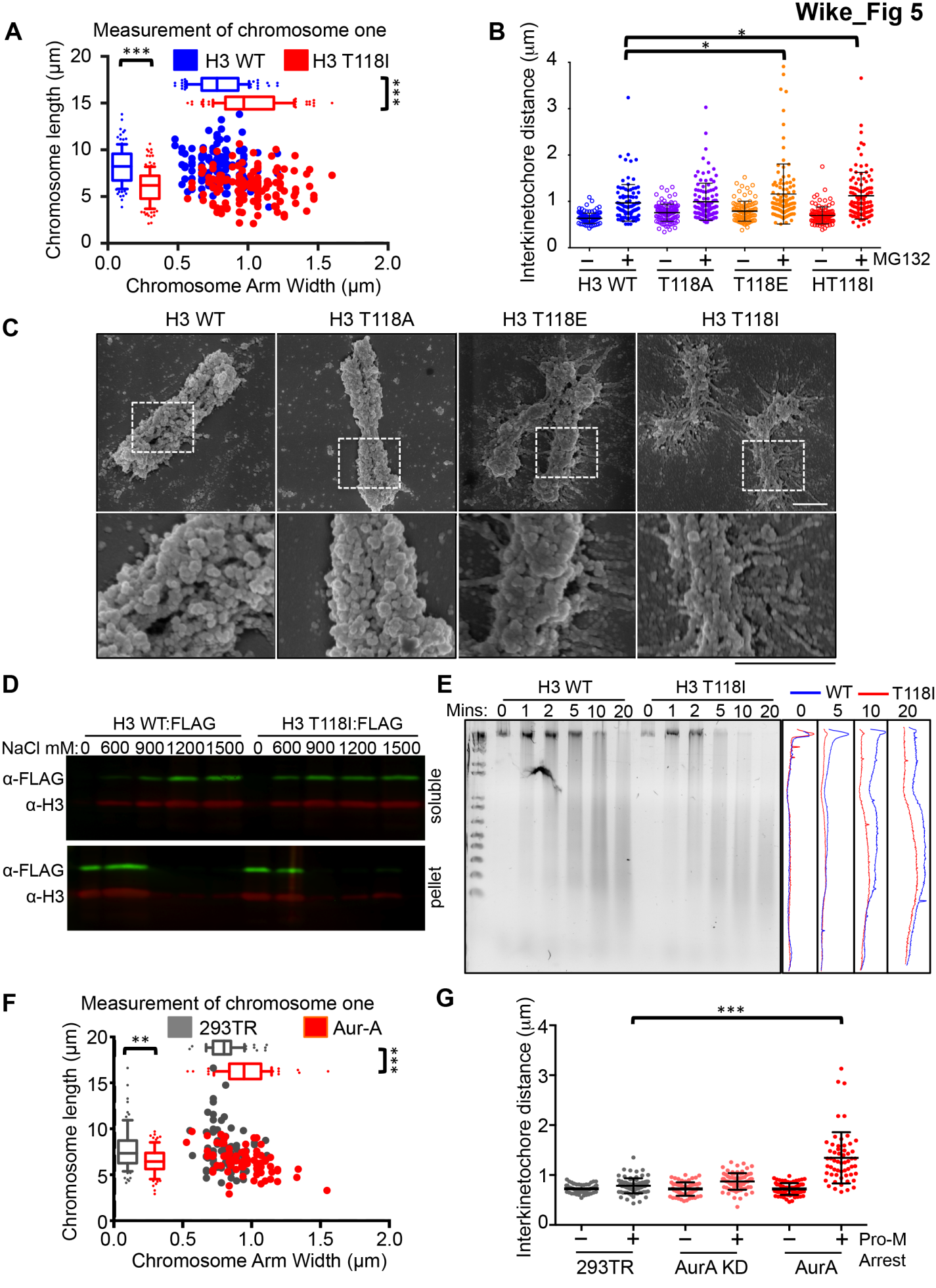
A
Measurement of chromosome one
H3 WT
H3 T118I
***
**
Chromosome length (μm)
Chromosome Arm Width (μm)
B
Interkinetochore distance (μm)
H3 WT
T118A
T118E
HT118I
MG132
C
H3 WT
H3 T118A
H3 T118E
H3 T118I
D
H3 WT:FLAG
H3 T118I:FLAG
NaCl mM: 0 600 900 1200 1500 0 600 900 1200 1500
α-FLAG
α-H3
soluble
pellet
E
H3 WT
H3 T118I
Mins: 0 1 2 5 10 20 0 1 2 5 10 20
WT
T118I
0 5 10 20
F
Measurement of chromosome one
293TR
Aur-A
**
Chromosome length (μm)
Chromosome Arm Width (μm)
G
***
Interkinetochore distance (μm)
293TR
AurA KD
AurA
Pro-M Arrest

Wike_Fig. 6

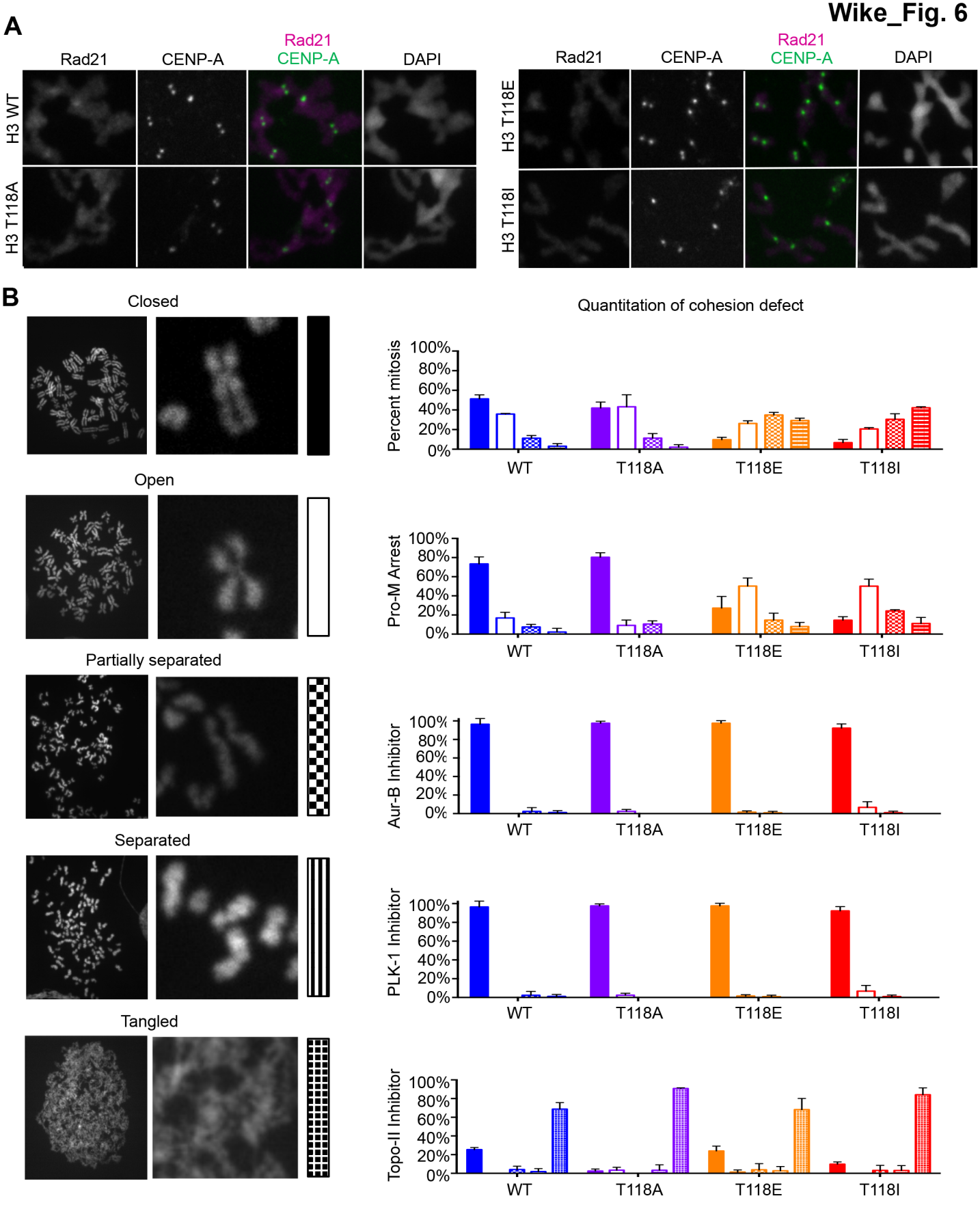
A
Rad21
CENP-A
Rad21
CENP-A
DAPI
H3 WT
H3 T118A
H3 T118E
H3 T118I
B
Closed
Open
Partially separated
Separated
Tangled
Quantitation of cohesion defect
Percent mitosis
Pro-M Arrest
Aur-B Inhibitor
PLK-1 Inhibitor
Topo-II Inhibitor
100%
80%
60%
40%
20%
0%
WT
T118A
T118E
T118I

Wike_Fig. 7

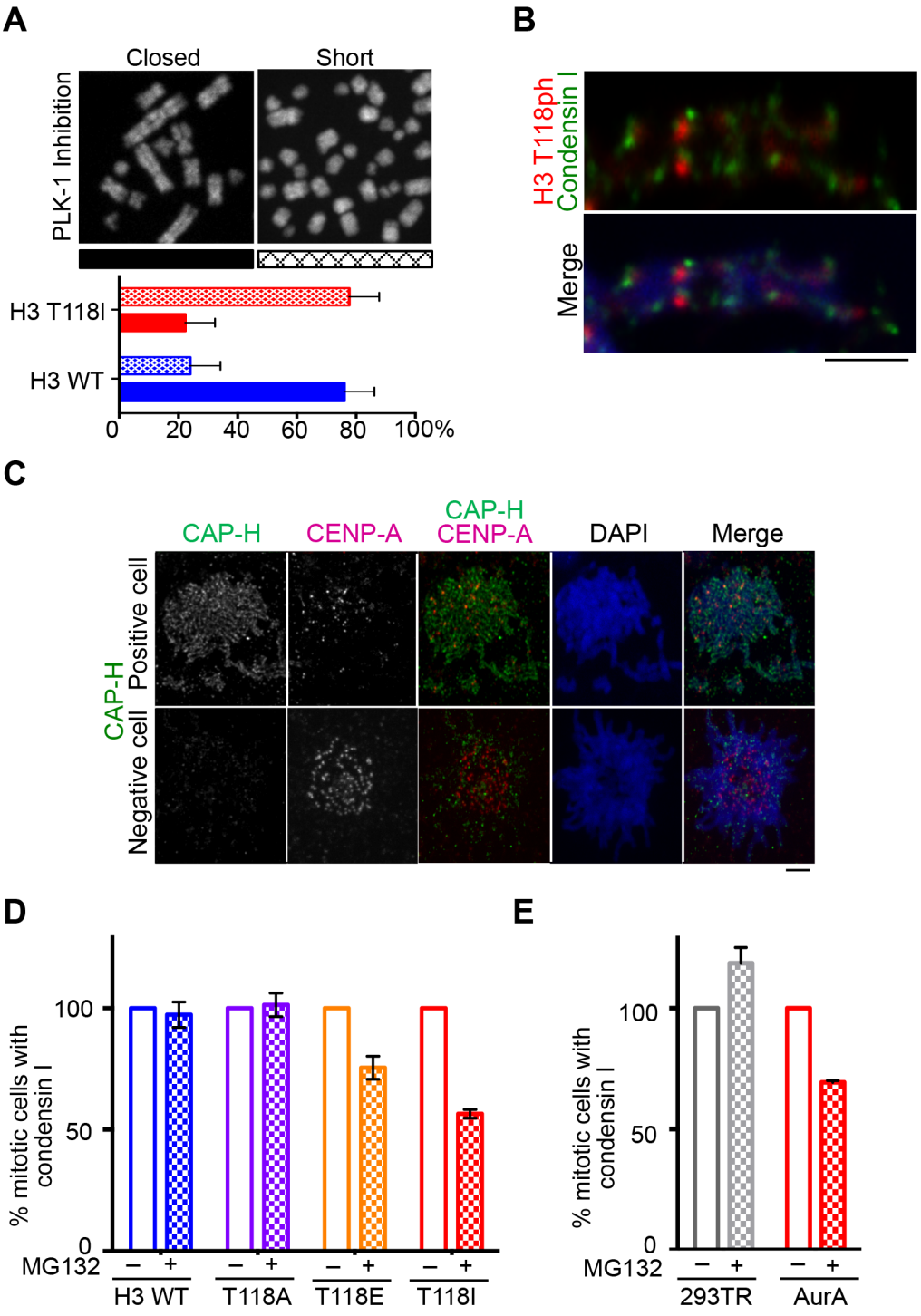
A
Closed
Short
PLK-1 Inhibition
H3 T118I
H3 WT
0
20
40
60
80
100%
B
H3 T118ph
Condensin I
Merge
C
CAP-H
CENP-A
CAP-H
CENP-A
DAPI
Merge
CAP-H
Positive cell
Negative cell
D
% mitotic cells with condensin I
100
50
0
MG132
–
+
H3 WT
T118A
T118E
T118I
E
% mitotic cells with condensin I
100
50
0
MG132
–
+
293TR
AurA

Wike_ Fig 8

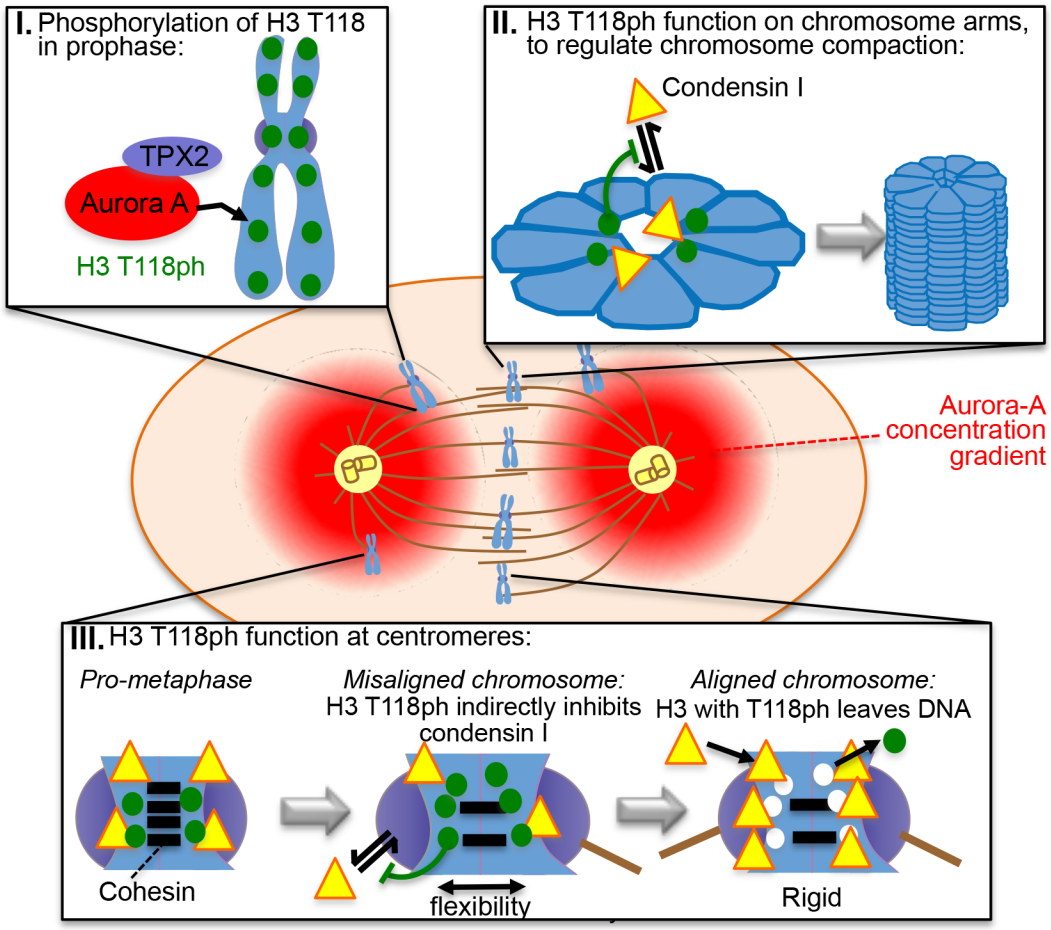
I. Phosphorylation of H3 T118 in prophase:
TPX2
Aurora A
H3 T118ph
II. H3 T118ph function on chromosome arms, to regulate chromosome compaction:
Condensin I
Aurora-A concentration gradient
III. H3 T118ph function at centromeres:
Pro-metaphase
Misaligned chromosome:
H3 T118ph indirectly inhibits condensin I
Aligned chromosome:
H3 with T118ph leaves DNA
Cohesin
flexibility
Rigid